

The Biggest Megaraptoridae (Theropoda: Coelurosauria) of South America

Alexis M. Aranciaga Rolando (✉ mauro.a_guido@hotmail.com)

Museo Argentino de Ciencias Naturales “Bernardino Rivadavia” (CONICET)

Matias J. Motta

Museo Argentino de Ciencias Naturales “Bernardino Rivadavia” (CONICET)

Federico L. Agnolín

Fundación de Historia Natural “Félix de Azara”, CEBBAD - Universidad Maimónides

Makoto Manabe

Natural Museum of Naure & Science

Takanobu Tsuihiji

Natural Museum of Naure & Science

Fernando E. Novas

Museo Argentino de Ciencias Naturales “Bernardino Rivadavia” (CONICET)

Research Article

Keywords: Megaraptoridae, Maastrichtian, South America, Patagonia

Posted Date: December 22nd, 2021

DOI: <https://doi.org/10.21203/rs.3.rs-1152394/v1>

License:  This work is licensed under a Creative Commons Attribution 4.0 International License.

[Read Full License](#)

Abstract

Megaraptorans are a theropod clade distributed in former Gondwana landmasses and Asia. Most members of the clade are known from early Cretaceous to Turonian times whereas Maastrichtian megaraptorans are known just from isolated and poorly informative remains. The aim of present contribution is to describe a partial skeleton of a megaraptorid coming from Maastrichtian beds at Santa Cruz province, Argentina. This new taxon constitutes the most informative megaraptoran from post-Turonian beds. Phylogenetic analysis nested the new taxon together with South American megaraptorans in a monophyletic clade, whereas Australian and Asian members constitute successive stem groups. South American forms differ from more basal megaraptorans in several anatomical features and in being much larger and more robustly built. It is possible that the Cenomanian-Turonian extinction of carcharodontosaurids was allowed to megaraptorans to occupy the niche of top predators in South America.

Introduction

Megaraptorans are a group of predator dinosaurs that inhabited, in Asia, Australia and South America from Barremian to Maastrichtian times^{1-3, 5,6}. These theropods are diagnosed by their elongate skulls, presence of apicobasally short and strongly curved teeth, devoid of mesial denticles, and 8-shaped in cross section, highly pneumatic axial skeleton reaching to the mid-caudal vertebrae, and long and powerful arms bearing large and sharp manual claws on digits I and II^{1,2,6-14}.

Although some authors^{1,15,16} interpreted megaraptorans as an archaic group of allosauroid theropods, increasing evidence lends support to the hypothesis that they are, instead, members of Coelurosauria^{2,4,10,12,17-20}. Aside from the consensus currently arrived on the phylogenetic allocation of Megaraptora among Coelurosauria, the internal relations of this clade remain poorly solved or unsolved at all.

The record of Megaraptora in Asia corresponds to Upper Barremian sediments of Shao Khua Formation in Thailand (*Phuwiangvenator* and *Vayuraptor*,^{4, 5}) and from Upper Barremian Kitadani Formation in Japan (*Fukuiraptor*,²¹). In Australia, the oldest records are from Barremian-Aptian rocks of the Strzelecki Group²², followed by those of the Albian Eumeralla Formation (*cf. Australovenator wintonensis*,^{22,23}). The Grimman Creek Formation (Mid Albian) also yielded megaraptorid remains (*Rapator ornitholestoides*, and two indeterminate megaraptorids,^{24,25}). The youngest records for Megaraptoridae is from the Winton Formation (Cenomanian–?Turonian) as represented by *Australovenator wintonensis* and an indeterminate megaraptoran²⁶⁻²⁸.

As concerned for South America, the oldest record of a probable megaraptoran comes from the Albian Santana Formation²⁹. An isolated caudal centrum of an indeterminate megaraptorid was also reported from the Late Cretaceous of Mato Grosso, Brazil (Late Cretaceous;³⁰).

Patagonia has the richest megaraptorid record of the continent. The oldest Patagonian records are an indeterminate megaraptorid coming from Bajo Barreal Formation (Cenomanian-Turonian;²⁰) and *Aoniraptor libertatem* found in beds of the Huincul Formation (Cenomanian-Turonian;^{13,31}). The following records are, in temporal order, *Megaraptor namunhuaiquii* from the Portezuelo Formation (Coniacian;^{6,10,17}), *Murusraptor barrosaensis* from the Sierra Barrosa Formation (Coniacian;³²), *Aerosteon riocoloradensis* from the Anacleto Formation (Santonian;³³), *Tratayenia rosalesi* from the Bajo de la Carpá formation (Santonian;¹⁹), *Orkoraptor burkei* from the Cerro Fortaleza Formation (Campanian;³⁴), some indeterminate megaraptorid remains from the Maastrichtian Lago Colhué Huapi^{35,36} and isolated teeth from Chorrillo Formation³.

The aim of the present contribution is to describe a new species of big-sized megaraptorid from Campanian-Lower Maastrichtian Chorrillo Formation in SW Santa Cruz province, Argentina, which constitutes one of the youngest records for the entire group. The new materials invite to examine the thoracic anatomy of megaraptorids, as well as review some aspects of the evolutionary radiation of carnivorous dinosaurs during the Upper Cretaceous in Gondwana.

Institutional abbreviations. **MACN-CH**: Museo Argentino de Ciencias Naturales “Bernardino Rivadavia”, Colección Chubut, Ciudad Autónoma de Buenos Aires, Argentina; **MPM**: Museo Padre Molina, Río Gallegos, Santa Cruz, Argentina.

SYSTEMATIC PALAEOLOGY

Theropoda Marsh, 1881

Tetanurae Gauthier, 1986

Coelurosauria von Huene, 1920

Megaraptora Benson et al., 2010

Megaraptoridae Novas et al., 2013

Maip macrothorax gen. et sp. nov.

Zoo bank registration: urn:lsid:zoobank.org:pub:E447F58E-28D6-4CFD-B5E3-BC4009DE5423

Derivation of name. *Maip* (Fig. 1A) is an evil entity from the Aonikenk mythology that represents “the shadow of the death” which “kills with cold wind”, and roams in the Andes mountains. The specific name, *macro*, derives from the Latin “big” and “thorax” refers to its wide thoracic cavity (which has, approximately, more than 1.20 m width) (Fig. 1B).

Holotype. MPM 21545, including axis, dorsals 2, 3, 4, 5, 6, 7, 9 and 10 (or 11), two proximal caudals (caudal A, probably pertaining to caudal 3-5 and caudal B, pertaining to caudal 6-8), three incomplete

cervical ribs, numerous incomplete or fragmentary dorsal ribs, numerous gastral elements, left coracoid, fragments of the scapula, and plus the elements already described in Novas *et al.*³, including the centrum of D12 or D13, proximal caudal, a proximal pubis and distal end of a second metatarsal (Fig. 1A). The specimen was found associated, but not in articulation, in a 5x3 m surface area, and no more than 1m thick bed (Fig. 1C).

Locality. Megaraptorid Site (Locality 3; see Novas *et al.*³), La Anita Farm, 30 km West from El Calafate city, Santa Cruz province, Argentina. Chorrillo Formation (Maastrichtian;^{3,37,38}).

Diagnosis. Megaraptorid theropod diagnosable on the basis of the following combination of characters (autapomorphies marked by an asterisk): 1) mid-dorsal vertebrae with articular surface of parapophyses saddle-shaped (absent in *Aerosteon* and *Murusraptor*)*; 2) mid-caudal vertebrae with an accessory posterior centrodiapophyseal lamina that subdivides the postzygapophyseal-centrodiapophyseal fossa in two pneumatic fossae (absent in *Aoniraptor*, *Aerosteon*, *Megaraptor*, and *Orkoraptor*)*; 3) first dorsal rib with honey-comb internal structure on its tubercle (absent in *Australovenator*, *Megaraptor*, and *Murusraptor*); 4) prominent anterior projection on the coracoid (absent in *Fukuiraptor*, *Aerosteon*, and *Megaraptor*)*; 5) coracoid without a subglenoid ridge (subglenoid ridge present in *Aerosteon*)*; 6) coracoid without a posteroventral fossa (posteroventral fossa present in *Fukuiraptor*, *Aerosteon*, and *Megaraptor*); and 7) and coracoid with ventromedial margin forming a dorsoventrally deep articular surface for the sternum (absent in *Fukuiraptor*, *Aerosteon*, and *Megaraptor*)*.

Results

Some bones of holotype of *Maip macrothorax* have been previously described by Novas *et al.*³, thus we refer to this paper for such materials. The dorsal centrum originally described as belonging to a “posterior dorsal” is here reassigned to dorsal 13th.

Based on comparisons with the complete cervico-dorsal sequence preserved in a juvenile specimen of *Megaraptor namunhuaiquii*¹⁰, and holotypes of *Aerosteon riocoloradensis*^{14,33}, *Murusraptor barrosaensis*^{12,32}, and *Tratayenia rosalesi*¹⁹, the cervico-dorsal series of *Maip macrothorax* is represented by the axis (Fig. 2), D2 through D7, D9, D10 or D11, D12, and D13 (Fig. 3-8). Only three caudals are currently known for *Maip macrothorax*, corresponding to the proximal third of the tail, which can be compared with proximal caudals of *Megaraptor namunhuaiquii*¹⁰, *Orkoraptor burkei*³⁴, and *Aerosteon riocoloradensis*^{14,33}. Holotype of *Maip macrothorax* also preserves several ribs tentatively referred as cervicals 5, 7 and 8 (Fig. 10), and dorsals 1, 2, and 6, as well as many other indeterminate rib fragments (Fig. 11). Many lateral and medial gastral elements have been recovered, probably belonging to the anterior half of the chest (Fig. 12). As it is observed in other megaraptorids, *Maip macrothorax* exhibits proportionately low cervicals (as represented in this case for the axis) as compared with posterior dorsals, which are twice the height of anterior cervicals. The axial elements available for *Maip* expand the knowledge on axial anatomy in Megaraptoridae, offering novel anatomical information on axis, anterior

dorsal series, cervical and dorsal ribs, anterior medial and lateral gastral elements, which remain unknown in other megaraptorids.

Axis: The axis is almost complete (Fig. 2), only lacks its right postzygapophysis and both prezygapophyses. In lateral view (Fig. 2 A), it is taller than long, being the neural arch almost two times the height of the centrum. The neural spine is low but robust, being less than half of the height of the neural arch. The intercentrum exhibits a rugose texture; it is placed below (not anteriorly) to the pleurocentrum, and immediately ventral to the parapophyses. The intercentrum is subtriangular in lateral view, and shows a moderate laterodorsal projection. Anteriorly, the intercentrum is crescent-shaped and anteriorly concave; it is subtriangular in contour in ventral view. The pleurocentrum shows an irregular anterior surface, the odontoid process being damaged. The pleurocentrum is squared-shaped in lateral view, being slightly taller than long. It is laterally concave and shows an anteroposteriorly large, deep oval depression, perforated by a single pneumatopore (on both sides of the centrum). The centrum is rounded and moderately concave. The posterior articular surface is wider than its anterior counterpart. A broken ventral margin of centrum reveals a camellate internal structure. The parapophyses are small, oval in contour (dorsoventrally higher than anteroposteriorly long), slightly concave and placed on the anterior margin of centrum.

The neurocentral suture is irregular. The transverse process is short, lateroventrally oriented and close to the anterior margin of the vertebra. A moderately developed, obliquely oriented postzygodiapophyseal lamina is observed. This crest delimits a postzygapophyseal-centrodiapophyseal fossa which exhibits a single pneumatic opening on its center. The postzygapophyses are concave and anteroposteriorly long in lateral view; in posterior aspect they are notably mediolaterally wide and its articular surface is ventrally concave and strongly laterally projected. The postzygapophyses bear oval (wider than long) articular surfaces. The interpostzygapophyseal lamina is stout and dorsally concave. Posteriorly, the neural arch shows a deep and anteroposteriorly long spinopostzygapophyseal fossa. This pneumatic fossa is deep and subtriangular-shaped. The spinopostzygapophyseal laminae are stout, dorsally concave and reach the tip of the neural spine. The spinopostzygapophyseal lamina diverges posteriorly.

The epipophyses are stout, dorsoventrally low, and mediolaterally wide. They are subtriangular in side view, and posteriorly do not surpass the posterior level of centrum. In anterior view, the neural canal is subtriangular, but it is oval and notably wider than tall in posterior view. The latter is dorsoventrally short but transversally wide. The neural spine is squared-shaped and low in side aspect. The anterior margin of the neural spine is broken, but it is evident that it is much thinner than the posterior margin, conferring a subtriangular cross-section to the neural spine. The intervertebral ligament rugosity is weak.

Dorsal vertebrae

D2: It is represented by an incomplete neural arch (Fig. 3). The neural spine and the right transverse process are only preserved at its base.

This element is referred to D2 because of the presence of a strong and laterally facing prezygapophyseal-centrodiapophyseal fossa, prominent centroprezygapophyseal lamina, parapophyses placed partially on the centrum and transverse process anterior oriented, as it also occurs in D2 of *Megaraptor namunhuaiquii*¹⁰ and *Murusraptor barrosaensis*^{12,32}.

The neurocentral suture is ventrally convex. Only the roof of the parapophysis is placed in the neural arch indicating its anterior position on the column. The articular surface of the parapophysis is concave. In lateral view, the left transverse process is subhorizontally oriented due to breakage, while the left process is dorsally oriented, which seems to be its original morphology. In dorsal view, the transverse process is subrectangular-shaped (with subparallel anterior and posterior margins), anteroposteriorly long, and slightly posteriorly oriented. On its posterior surface, this process shows a deep and oval pneumatic opening located at its mid-length. Ventral to this process there are three well-developed laminae. The centroprezygapophyseal lamina more anteriorly, the anterior centrodiapophyseal lamina in the middle and the posterior centrodiapophyseal lamina more posteriorly. Between the centroprezygapophyseal and the anterior centrodiapophyseal lamina is observed the prezygapophyseal-centrodiapophyseal fossa, which is subtriangular and pneumatic in nature. The anterior and posterior centrodiapophyseal laminae delimit the centrodiapophyseal fossa, which is subtriangular in shape and ventrally facing. This fossa is asymmetric being pneumatic on the left side and apneumatic on the right. The posterior centrodiapophyseal lamina is stout and obliquely oriented. It forms the anterior limit of the postzygapophyseal-centrodiapophyseal fossa, which is deep and probably pneumatic. The transverse process shows a big, round, concave and laterally (or slightly lateroventrally) facing diapophysis. It is surrounded by rugose surfaces which may correspond to the *lig. costotransversarium* attachments. The postzygapophyses face posteroventrally and are placed slightly below the prezygapophyses. In ventral view, the articular surface of the postzygapophyses is oval (wider than long) in contour and flat or slightly concave. More dorsally, the spinopostzygapophyseal laminae are notably thick and stout. These laminae delimit the spinopostzygapophyseal fossa. This is subrectangular in shape and exhibits subtle intervertebral ligament tuberosity. Furthermore, this fossa is deep but, in this vertebra (but other anterior dorsal), the slope of such structure shows a step and do not falls abruptly as in more posterior vertebrae. The prezygapophyses are strongly anterior- or anterodorsally facing. Its articular surfaces are round, flat and slightly medially inclined. The prezygodiapophyseal lamina is sharp, sub-horizontally oriented and ventrally concave. In anterior view, the prespinal fossa is deep and strongly pneumatic. This fossa shows a wide pneumatic recess that communicates with at least three pneumatic foramina that enter into the bone. Ventral to the prezygapophyses, the centroprezygapophyseal lamina is laterally convex and there is an oval shaped and pneumatic centroprezygapophyseal fossa. This fossa is delimited medially by a sharp margin. The base of the neural spine is transversely wide. The intervertebral ligament tuberosity is weak, and becomes progressively transversely wider towards the top of the neural spine.

D3: This element preserves a partial neural arch with a right transverse process (Fig. 4 A-E). The postzygapophyses are partially preserved. The neural spine is broken but some fragments are observed at the base of the transverse process.

This element referred as a D3 based on the presence of a subhorizontally oriented transverse process (similar to D3 of *Murusraptor* and D2 of *Maip*; the transverse process of D4 is more dorsally oriented in *Aerosteon*), proximodistally short transverse process (shorter than D4 of *Aerosteon* but comparable to D3 of *Murusraptor*), laterally oriented transverse process in dorsal view (similar to D3 of *Murusraptor* but contrasting with the anteriorly projected process of D2 of *Maip*), and anteroposteriorly expanded tips of the transverse process (similar to D3 of *Murusraptor*).

The transverse process is slightly dorsally upturned but much less than in more posterior vertebrae. The transverse process is subrectangular in contour, and expands transversely close to its tip; a condition that does not occur in more posterior dorsals. This process is proximodistally short when compared with more posterior vertebrae. The dorsal surface is smooth with some thin longitudinal striations and some rugosities close to its tip. The articular surface of the diapophyses faces ventrally. The postzygapophysis shows a nearly flat articular surface. Dorsal to it, the base of the spinopostzygapophyseal lamina is stout and medially concave. The spinopostzygapophyseal fossa is deep and shows a step (as in D2 but contrasting with D6). The postzygapophyseal-centrodiapophyseal fossa is poorly preserved but shows, immediately anterior to the postzygapophyses, a deep penetrating pneumatopore. The broken walls of the vertebra show a camellate internal structure.

D4: It is represented by an isolated centrum (Fig. 4 F-I). This element is identified as the fourth because part of the parapophysis is placed in the neural arch, a single squared or round pneumatopore, as well as the absence of a ventral keel, a condition retained in the first dorsal elements of theropods (such as D1 of *Aerosteon*).

The centrum is round or subrectangular being slightly dorsoventrally taller than anteroposteriorly long and with sub-parallel anterior and posterior surfaces. Its ventral and lateral margins are shallowly concave. The posterior articular surface of the centrum is incompletely preserved but seems to be deeply concave, which suggests that the centrum was opisthocoelous. The anterior articular surface of centrum is almost flat and slightly taller than wide. The ventral margin lacks a keel or longitudinal groove is almost smooth and its anterior surface is strongly rugose. In lateral view, the centrum is longitudinally concave and smooth. At mid-height it shows a deep and round pneumatopore, placed within a shallow pneumatofossa. Anteriorly, the parapophyses is ovoidal in contour, dorsoventrally taller than anteroposteriorly long. The parapophyses show a rugose surface that may represent the attachment of the *lig. costovertebral*, which connects the parapophyses with the capitulum of the rib, as occurs in extant bird³⁹.

D5: It is represented by a fragmentary neural arch, preserving the right prezygapophysis and the base of the right transverse process (Fig. 5 A, C-E).

Is interpreted as a D5 because of the presence of an anterior centrodiapophyseal lamina stouter than in D6, a slightly bigger centrodiapophyseal fossa than in D6, and a slightly smaller parapophysis than that present in D6.

In side view, there are the bases of both centrodiapophyseal laminae. The posterior centrodiapophyseal lamina seems stout. The anterior centrodiapophyseal lamina is thin but not as thin as in more posterior dorsal vertebrae. The centrodiapophyseal fossa is deep, subtriangular in contour and exhibits a pneumatopore that penetrates the vertebra. The prezygapophyses are short and stout, and its articular surface is subtriangular in contour. The articular surface is flat to slightly convex and slightly medially facing. The centroprezygapophyseal lamina is located ventral to the prezygapophyses. This lamina is relatively short, straight, anteroposteriorly oriented and delimits the medial side of the centroprezygapophyseal fossa. This fossa is subcircular in contour and deep. The parapophyses are notably wide and, as in D6, the articular surface is sigmoidal in contour. Located between the anterior centrodiapophyseal lamina and the prezygapophyses an oval and deep pneumatopore is present.

D6: This vertebra is represented by an incomplete neural arch, the right transverse process, the postzygapophyses and the base of the neural spine (Fig. 5 B, F-I). The tip of the transverse process and diapophyses are incompletely preserved. Damaged parts of the bone reveal an internal pneumatic camellate structure.

It is identified as a D6 because of the following characters: parapophyses placed between the centrum and neural arch (placed in the centrum in D3 of *Murusraptor* and D4 of *Aerosteon* but placed in the neural arch in D7 of *Murusraptor* and D8 of *Aerosteon* and *Murusraptor*). The anterior centrodiapophyseal lamina is much shorter than the posterior one (subequal in length at the anteriormost dorsals of other Megaraptoridae but absent posterior to 10th dorsal). Transverse process slightly dorsally oriented (laterally oriented in D3 of *Murusraptor* and D4 of *Aerosteon* but more strongly dorsally oriented in D7 of *Murusraptor* and D8 of *Aerosteon* and *Murusraptor*).

In lateral view, the transverse process is upturned and slightly anteriorly oriented. It is subtriangular in contour and with subparallel anterior and posterior margins that smoothly converged toward the base. The articular surface of the process is rounded in contour, slightly concave and lateroventrally facing. The process shows a rugose anterior surface that probably constitutes the insertion of the ligaments that attaches the rib with the vertebra³⁹. Posteriorly, the transverse process shows at least three pneumatic foramina closer to its tip. The postzygapophyseal-centrodiapophyseal lamina is notably stout and subvertically oriented. This lamina dorsally delimits a deep postzygapophyseal-centrodiapophyseal fossa which shows a pneumatopore just anterior to the postzygapophyses. This fossa occupies the preserved posterior surface of the neural arch. Ventral to this surface and placed between the centrodiapophyseal laminae there is a strongly rugose surface covered with round pits as well as a pair of foramina, which constitutes the insertion of the *lig. costotransversarium* joining the transverse process with the tubercle of the rib, as documented by non-avian theropods and extant birds³⁹. Ventral to the transverse process there are two laminae delimiting three fossae. The posterior postzygapophyseal-centrodiapophyseal fossa, is deep and pneumatic in nature because presence of two strong pneumatopores below the postzygapophyses. The posterior centrodiapophyseal lamina is long, robust and slightly posteriorly concave. Close to the tip of the transverse process, this lamina connects with the rugose surface that constitutes the insertion of the *lig. costotransversarium*. This rugose surface is delimited by a small and

round concavity. The anterior centrodiapophyseal lamina is notably thinner and shorter than other laminae, representing one third of the thickness of the posterior centrodiapophyseal lamina. The centrodiapophyseal fossa is subtriangular in contour, deep and exhibits two pneumatopores: one subrectangular and placed dorsal to the parapophyses and the other one ovoid in contour and placed between the junctions of both centrodiapophyseal laminae. Anteriorly to the centrodiapophyseal lamina the prezygodiapophyseal lamina is placed. It is subvertically oriented, deep and nearly straight. Separating this lamina from the anterior centrodiapophyseal lamina, is located the prezygapophyseal-centrodiapophyseal fossa. It is deep, subrectangular in contour and pneumatic in nature. The parapophyses are subcircular in contour and relatively large, occupying almost two thirds of the anteroposterior length of the neural arch. The parapophyses are asymmetrical in shape (probably due to tafonomic causes); the one of the right side is saddle-shaped whereas the left one is cup-shaped. Saddle shaped parapophyses constitutes an autapomorphy of this species. The parapophyses exhibits an internal camellate structure. The articular surfaces of the postzygapophyses are rounded or squared in contour. The right postzygapophysis shows a pneumatic foramen on its posterior margin. The spinopostzygapophyseal laminae are thick and laterally concave. They are separated by a deep, subtriangular-shaped spinopostzygapophyseal fossa. The hyposphene is broken and shows a pneumatic foramen on its right side.

There are well-developed centroprezygapophyseal lamina. It is proximodistally short, lateroventrally oriented and reaches the lateral margin of the neural arch. Ventrally to the prezygapophyses there is a subcircular and deep centroprezygapophyseal fossa. The prespinal fossa is poorly preserved. The neural canal is subcircular in contour and taller than wide. The hypantrum is very wide and deep. A moderate intervertebral ligament tuberosity is observed on the posterior surface of the neural spine. These tuberosities are thinner ventrally but become progressively transversally wider dorsally.

D7: This element is represented by a partial neural arch exhibiting a complete left transverse process and the left postzygapophyses (Fig. 6). Some broken parts reveal an internal camellate structure.

It is identified as the seventh dorsal because of the presence of: a moderately upturned transverse processes (less dorsally projected than D8 of *Aerosteon* or D7 and D8 of *Murusraptor* but similar to D6 described above); a transversely thin hyposphene (thinner than in D4 of *Aerosteon* but comparable to D8 of *Aerosteon* and D7 of *Murusraptor*); and deep, abruptly excavated and moderately narrow spinopostzygapophyseal fossa (much deep and narrow than D4 of *Aerosteon* and D6 of *Maip* and shallower and wider than D8 of *Aerosteon* and D7 and D8 of *Murusraptor*).

The transverse process of this element is notably upturned, long and subtriangular in outline when viewed from the side. In dorsal view, the transverse process shows nearly straight and subparallel anterior and posterior margins, resulting in a subrectangular contour. Close to the lateral margin, both margins are slightly expanded. The expanded distal end of the transverse process is rugose, probably representing muscular or ligament attachments. The articular surface of the diapophysis is lateroventrally facing and shows a subtriangular rugosity immediately ventrally for the attachment of the *lig.*

costotransversarium. The posterior centrodiaepophyseal lamina is wide and straight. The postzygodiaepophyseal lamina is stout. The postzygapophyseal-centrodiaepophyseal fossa is deep and close to its dorsal margin it shows small foramina of probable neurovascular nature. Anteromedial to the postzygapophyses, a set of small pneumatic cavities is present. In addition, deeply in the postzygapophyseal-centrodiaepophyseal fossa are observed two pneumatic channels. One posterior, which connects the postzygapophyses each other and one anterior which gets into the bone.

The postzygapophysis shows a nearly flat articular surface. The hyposphene is transversely thin and dorsoventrally tall (taller than in D6). The spinopostzygapophyseal fossa, dorsally delimits the postzygapophyses. It is notably deep, and subtriangular in contour. In anterior view, the prezygodiaepophyseal lamina is thick and straight.

D9: It is represented by a nearly complete element. The neural spine is notably distorted and its top is not complete. The neural arch lacks the tips of the right transverse process (Fig. 7) and the right postzygapophyses is broken. The centrum is incomplete and distorted on its posterior half. Broken areas show an internal camellate structure.

It is identified as a D9 because of the presence of dorsally upturned and long transverse processes (observed in D10 and D11 of *Aerosteon*), anteroposteriorly stout transverse process (stouter than D7 of *Maip* and D8 of *Aerosteon* but resembling D10 of the same taxa), parapophyses placed entirely in the neural arch (a condition present in the distal half of the dorsal series), presence of a stout posterior centrodiaepophyseal lamina and weak anterior centrodiaepophyseal lamina (observed in D8 of *Aerosteon* but not in D10), the centrum shows a taller than wide anterior articular surface, which is only observed in D8 of *Aerosteon* (but not in more distal dorsals).

In lateral view, the transverse process is strongly upturned and perpendicularly oriented with respect to the anteroposterior axis of the vertebra (both features contrast with D6-7 of *Maip* which shows moderately upturned and slightly posteriorly oriented transverse process). In cross section, the transverse process is subtriangular in contour and exhibits subparallel anterior and posterior margins. The articular surface of the diapophysis is oval in contour (anteroposteriorly longer than dorsoventrally high), slightly concave and lateroventrally facing. Anteriorly, the transverse process shows a stout, prominent and dorsally concave spinodiaepophyseal lamina. Laterally, such lamina becomes anteroposteriorly lower, rugose and dorsoventrally expanded. Ventrally, this lamina is connected with a short prezygodiaepophyseal lamina. This lamina is "L" shaped in lateral view and shows a small projection closer to its anterodorsal margin. Close to its tip, the transverse process shows strong transversal striations along its anterior, dorsal and posterior margins. The diapophyses are surrounded by rugosities. These striations and rugosities probably constitute the insertion of the *lig. Costotransversarium*³⁹. The diapophyses show a strong and rugose ventral projection that shows concave anterior and posterior surfaces. The projection and concave surfaces represent the ventral insertion of the *lig. costotransversarium*³⁹. Posteriorly, the transverse process shows a postzygodiaepophyseal lamina. This lamina is straight laterally but, on its medial half, the shaft of this lamina becomes ventrally curved when viewed posteriorly. At mid-length to the

transverse process, it is observed an oval and drop-shaped surface which encloses at least two oval foramina. Lateroventrally, this drop-shaped surface is delimited by a raised, slender and rugose area. Ventrally, the transverse process shows anterior and posterior centrodiapophyseal laminae. The posterior one is notably stouter than the anterior one. On both sides of the vertebra, the laminae are asymmetrical in shape, at the left side the posterior centrodiapophyseal lamina shows a subtriangular ventral half that is not present at the right side. The anterior centrodiapophyseal lamina is reduced and more ventrally placed on the left side of the vertebra. Both laminae delimit the prezygapophyseal-centrodiapophyseal, the centrodiapophyseal and the postzygapophyseal-centrodiapophyseal fossae. All are very deep and pneumatic. The centrodiapophyseal fossa is also asymmetrical being notably reduced on the left side but much wider on the right one. On this side, it shows three pneumatic openings. The parapophyses are large and rounded in contour, occupying almost half the anteroposterior length of the neural arch. The parapophyses are asymmetrical being saddle-shaped on the right side and cup-shaped on the left one. The anterior margin of the right parapophysis is rugose. It is posterodorsally delimited by a concave, smooth and obliquely oriented surface that probably represents the insertion of the costovertebral ligament³⁹. The articular surfaces of the postzygapophyses are round or subrectangular, ventrally concave and smooth. The hyposphene is transversely thin and dorsoventrally high. The spinopostzygapophyseal laminae are stout and laterally concave. They are separated by a deep, pneumatic and subtriangular spinopostzygapophyseal fossa.

The prezygapophyses are stout and strongly anteriorly projected. Its articular surface is subtriangular in contour, nearly flat and dorsally oriented. Medial to the base of the prezygapophyses there is a small, and probably pneumatic in nature, foramen. Ventral to the prezygapophysis is a well-developed centroprezygapophyseal lamina. Such lamina is short and stout, it is lateroventrally oriented and reaches the lateral margin of the neural arch. Ventral to the prezygapophyses a subcircular and deep centroprezygapophyseal fossa is present. The hypantrum is wide and deep. The neural canal is ovoidal in contour, dorsoventrally taller than transversely wide. The prespinal fossa is deep, subtriangular in contour and pneumatic. The prespinal lamina is thick and slightly ventrally expanded. The prespinal lamina, together with the spinodiapophyseal and the prezygodiapophyseal laminae, delimit a subtriangular and deep accessory fossa. A notably anteriorly projected intervertebral ligament rugosity is observed on the anterior surface of the neural spine.

The vertebral centrum in lateral view is subrectangular in contour and slightly taller than long. Its lateral and ventral margins are deeply concave. The pleurofossa includes two pleurocoels. The anterior one is wide and suboval in contour (anteroposteriorly longer than dorsoventrally tall). The posterior pleurocoel is smaller and suboval in outline.

The anterior and posterior articular surfaces of centrum are strongly laterally projected and show striations for the attachment of the intervertebral ligaments. The posterior surface is nearly flat and the anterior one is concave. The ventral surface is smooth and shows numerous neurovascular foramina. The neurocentral suture is rugose and shows an internal camellate structure.

D10 or 11: This element consists of an isolated centrum, lacking the posterior articular surface and the posteroventral projection (Fig. 8). The posterior surface as well as the posteroventral projection are broken and show a camellate internal structure.

It is referred to D10 or D11 because of the presence of a strong projection of the lateral and ventral margins of its anterior and posterior articular surfaces (deeper than D8 of *Aerosteon* but similar to D10 of *Aerosteon* and D11 of *Murusraptor* and *Aerosteon*), a deep pleurocoel and a blind fossa immediately posterior to it (present in D10 and D11 of *Aerosteon* and D11 of *Murusraptor*). Novas *et al.*³ described an isolated dorsal centrum of *Maip*, which is referred here as D12 or 13 because of its large size, its strong transverse constriction of the centrum and its notably transversely wide anterior articular surface, a combination of characters observed in D13 of *Aerosteon*¹⁴. This element was described by Novas *et al.*³ and will not be described here.

In lateral view, the vertebral centrum of D10-11 is subrectangular in contour and longitudinally concave. The lateral wall is smooth with some obliquely oriented striations, representing the insertion of the intervertebral ligaments, close to the anterior and posterior articular surfaces. In anterior view, the centrum is oval in contour, being slightly taller than wide, and feebly concave. The ventral surface of the centrum is smooth and shows some neurovascular foramina. The anterior articular surface of the centrum is strongly ventrally projected.

In lateral view it shows a deep pleurofossa having an anterior pneumatopore and a posterior blind fossa, both separated by an oblique septum. The pneumatopore is very deep, oval in contour and much wider than the blind fossa.

Caudal vertebrae

Caudal vertebrae are represented by two well-preserved neural arches belonging to the most proximal part of the tail.

A proximal caudal is represented by its neural arch and neural spine, lacking the tip of the right transverse process. (Fig. 9 A-D). It is assigned to caudals between Ca3 and Ca5 because of the laterodorsal orientation of the transverse process, the strong height of the neural spine and the strong anterior projection of the pre- and postzygapophyses.

Transverse processes are long, subhorizontally oriented and strongly posteriorly projected. The left process is completely preserved and becomes dorsoventrally thicker towards its tip. It shows strong striations along its dorsal and ventral margins. On its anteroventral corner, the process shows an oval and rugose concavity that probably constitutes the insertion of the *m. ilio-ischiocaudalis*^{40,41}. Ventral, the transverse process shows two well-developed buttresses that form the anterior and posterior centrodiapophyseal laminae. The anterior centrodiapophyseal lamina separates, anteriorly, the prezygapophyseal-centrodiapophyseal fossa, which is subtriangular and pneumatic; and posteriorly, the centrodiapophyseal fossa, which is rounded in contour, pneumatic and striated. The posterior

centrodiapophyseal lamina delimits posteriorly the postzygapophyseal-centrodiapophyseal fossa, which is oval and shows a deep pneumatophore.

The articular surfaces of the postzygapophyses are ovoidal in contour and are lateroventrally facing. The postzygapophyseal-centrodiapophyseal fossa is subdivided by an oblique lamina not observed in other megaraptoran. The spinopostzygapophyseal laminae are stout and delimit a wide and pneumatic spinopostzygapophyseal fossa. The prezygapophyses are short, robust and slightly dorsally upturned. Its articular surface is ovoidal in contour and mediodorsally facing. The prespinal fossa is deep and transversely narrow, and within this fossa there is a subtriangular pneumatopore as occurs in *Aoniraptor*¹³. The neural spine is proximodistally tall, and becomes notably thick towards its top. The neural spine is strongly posteriorly inclined and shows well-developed intervertebral ligament rugosities. The neural spine exhibits internal camellate structure. A shallow groove extends along the anterolateral margin of the neural spine. This groove ends at the base of the neural spine in a shallow fossa. In posterior view, the neural canal is dorsoventrally taller than transversely wide.

A more distal caudal (between Ca6 and Ca8) is represented by an incomplete neural arch, which lacks the right transverse process, the postzygapophyses and part of the neural spine (Fig. 9 E-H). It is referred to the proximal region of the tail because of the presence of wide and strongly posteriorly oriented transverse process and a tall and subvertically oriented neural spine.

The transverse process is anteroposteriorly long, stout, subtriangular in cross section and strongly posteriorly directed. It becomes slightly thicker towards its tip. It shows longitudinally oriented striations close to its tip. On its anteroventral margin, the transverse process shows longitudinal rugosities and striations. Ventral to the transverse process there are short and relatively stout centrodiapophyseal laminae. They delimit the centrodiapophyseal fossa, which is ovoidal in contour, deep and pneumatic. Anteriorly, the prezygapophyseal-centrodiapophyseal fossa, which is smaller than the centrodiapophyseal fossa, subtriangular in contour and also pneumatic. It is dorsally delimited by the prezygodiapophyseal lamina, which is short and subhorizontally oriented. Posteriorly, the postzygapophyseal-centrodiapophyseal fossa is ovoidal in contour, relatively small and pneumatic. This latter fossa is and oval. Dorsal to this fossa, a short accessory posterior centrodiapophyseal lamina is present. This lamina is not observed in any other Megaraptora and may represent an autapomorphy of *Maip*. It delimits a blind and subtriangular-shaped concavity. The prezygapophyses are short, stout, and slightly upturned. The articular surfaces are slightly convex, show a subquadrangular contour, and are medially facing. The spinoprezygapophyseal lamina is transversely thin, dorsoventrally tall and subparallel to each other. The spinoprezygapophyseal fossa is deep and transversally narrow. The neural spine is transversally thin, tall and shows smooth lateral surfaces, with exception of a subtriangular-shaped and raised area at its mid-height and that is covered with striations, probably representing a muscle attachment. On its anterior surface, the neural spine shows subtle intervertebral ligament rugosities. The neural canal is ovoidal in contour, dorsoventrally taller than transversely wide.

Cervical ribs:

The **fifth cervical rib** is represented by its proximal end. It is assigned to CR5 on the basis of the presence of a short and small tubercle, absence of an anterior process, and presence of a large capitulum, a combination of features present in CR5 of *Allosaurus*, *Tyrannosaurus*^{42,43} and C5 of *Aerosteon* and C6 of *Megaraptor*.

The rib head is small compared with sixth and eighth cervical ribs. The lateral surface of the rib head is smooth. The tubercle is short, and shows slightly convergent margins towards the tip. It shows a convex articular surface that exhibits pneumatic foramina on its lateral margin. In anterior view, tubercle and capitulum form a right angle to each other. The capitulum is much anteroposteriorly wider but transversally shorter than the tubercle. The articular surface of the capitulum is flat or rugose and subquadrangular in contour. The anterior surface of the capitulum is eroded and shows a camellate internal structure. An anterior pneumatic fossa is deep, dorsoventrally high and suboval in outline. The ventral surface of the capitulum is smooth and shows pneumatic foramina close to its articular surface. Medially, a straight and thick transverse lamina connects the tubercle with the capitulum. The posterior pneumatic fossa is deep and ovoidal in contour. The shaft of the rib is rod-like and exhibits a longitudinal and striated concave area immediately posterior to the capitulum.

The **seventh cervical rib** only lacks its distal tip (Fig. 10 A-E). It is assigned to a CR7 on the basis of a well-developed proximal head (absent in anterior ribs); presence of a pointing and well-developed anterior process (present at the mid-length of the neck in *Allosaurus* and *Tyrannosaurus*); a prominent and strongly projected tubercle; a notably curved shaft (as in posterior ribs) and tubercle and capitulum forming a nearly right angle when viewed anteriorly (observed at the mid-length of the neck in *Allosaurus*).

The rib head is large, subtriangular in shape in lateral view and anteroposteriorly long. The lateral and ventral surfaces of the rib head are flat, decorated only with some small longitudinal striations. Medially, in cross-section the rib head is deeply concave being "C"-shaped on its anterior half while is straight and "I"-shaped more distally. The anterior process is subtriangular in contour and acute. Also, such process exhibits an almost straight ventral margin and a deeply concave anterior margin. The anterior pneumatic fossa is deep, subtriangular in contour and anteriorly facing. The tubercle is elongate, thick and rod-shaped, with nearly straight anterior and posterior margins. The tubercle is much longer and thinner than the capitulum. Its articular surface is laterodorsally facing, rounded in contour, slightly concave and rugose. Close to its articular surface, the tubercle shows a small and rugose concavity probably for the insertion of the *lig. costotransversarium*. In anterior view, the tubercle and the capitulum form an almost right angle. A stout transverse lamina with a concave dorsal margin connects both structures. This lamina is slightly posteriorly oriented. In medial view, this lamina is perforated by an opening that communicates the anterior pneumatic fossa with the posterior one (see below). The capitulum is slightly eroded, it is ovoidal in cross-section and shows a slightly saddle-shaped dorsally faced and rugose articular surface. The capitulum has longitudinal striations close to its articular surface. Posteriorly, the capitulum shows two ovoidal pneumatic foramina that are laterally delimited by a curved lamina that connects the capitulum with the rib shaft and, medially, with a thin and concave ridge. The capitulum

shows a camellate internal structure. The posterior pneumatic fossa is anteroposteriorly long and becomes shallower posteriorly.

Distally, the shaft of the rib is very thin and delicate and becomes abruptly dorsoventrally thinner and slightly dorsolaterally curved. The shaft shows some longitudinal striations close to the tip of the anterior process. In cross-section, the rib is proximally "V"-shaped and becomes ellipsoidal towards its distal half.

A **left cervical rib** probably corresponding to the C8 is almost completely preserved, it lacks its distal tip and part of its proximal head (Fig. 10 F-H). It is referred as CR8 in the basis of a notably elongate shaft (but shorter than the first dorsal rib), that is wider than in CR7 and that is ventrally curved (a condition observed in ribs of the base of the neck of other theropods⁴²), and a long and obliquely oriented tubercle.

The rib head is smaller than in the sixth rib. The tubercle is slightly anteriorly inclined and strongly offset from the rib head. The anterior margin of the tubercle is slightly concave and the posterior one is obliquely oriented, straight and dorsally oriented. The articular surface of the tubercle is convex. The medial surface shows rugosities close to its articular surface, which constitutes the attachment of the *lig. costotransversarium*. This articular surface shows a posteriorly facing and rugose concavity. Near the base of the tubercle, part of a pneumatic fossa (probably the posterior one) is preserved. At mid-length, the shaft becomes abruptly thin and rod-like and curves ventrally. This morphology occurs in the posterior half of the neck in other theropods⁴²⁻⁴⁴. The lateral surface of the rib shaft is flat and dorsoventrally tall anteriorly and becomes progressively shallow posteriorly. The medial margin of the shaft is nearly flat, with a longitudinal rugosity all along its dorsal margin.

Proximally the rib shaft is subrectangular in contour, being transversely compressed, and becomes subcircular in contour at its distal half.

Dorsal ribs:

A probable **first left dorsal rib** is almost completely preserved, lacking only its distal end (Fig. 11 A-C). It is identified as a first dorsal rib, because of a strong proximal concavity, a slightly medially concave shaft and the presence of one flange on its posterior side and two flanges on its anterior side.

The rib head is robust (much stouter than on the cervical ribs), it is anteroposteriorly wide and shows a long and dorsally upturned capitulum. The dorsal margin of the rib head is deeply concave; its medial margin is concave and has a dorsoventrally oriented and deep and narrow concavity. The dorsal margin of the rib head projects anteriorly forming an anteromedial flange. Below the tuberculum, the rib head inflates as a strong anteroposterior thickening. This thickening affects all the rib head and becomes progressively wider through the dorsal part of the head. In anterior view, the rib head shows dorsoventral oblique groove which is delimited by a subparallel ridge. Within this groove is observed a set of aligned pneumatopores. Such pneumatophores become progressively bigger dorsally forming a honey-comb structure. This condition is observed only in this theropod. The posterior surface of the rib head is covered with strong rugosities. Dorsally, the thickening of the rib head is strongly expanded being almost twice the

anteroposterior width of the articular surface of the tuberculum. This thickening shows a deep proximal concavity above the head. The tuberculum is dorsally projected, strongly anteroposteriorly thickened and exhibits a rugose articular surface. This surface is oval in contour, concave and dorsally facing. Laterally, the tuberculum shows a rugose bump which probably constitutes the insertion of the *lig.*

*costotransversarium*³⁹. At mid-height, the tuberculum shows two foramina within a deep and rugose concavity. The articular surface of the capitulum is rounded in contour. Along its ventral margin, the capitulum shows an anteriorly facing concavity covered by striations and rugosities, that probably represent the attachment of the *lig. costovertebrale*³⁹.

The rib shaft is almost straight and shows an anterior concavity delimited by anteromedial and anterolateral bony flanges. Posteriorly, the rib shaft shows a sharp posterolateral flange that becomes weaker and loses at the mid-height of the rib. The posterolateral flange delimits a posterior concavity.

Proximally, the rib shaft is "L"-shaped in cross section, and becomes ellipsoidal towards its distal end.

A **second right dorsal rib** is represented by its proximal end (Fig. 11 D-F). It is identified as a second rib because of the presence of a lateromedially long capitulum (longer than in DR1 of *Murusraptor* and *Australovenator* but shorter than in DR2-3 of *Australovenator*), a shallow proximal concavity (deeper than DR1 but similar to DR2-3 of *Australovenator*), and the presence of one posterior and two anterior longitudinal flanges on the rib shaft.

The rib head is a thin plate, concave at its central part but strongly concave ventrally and laterally. Dorsally, the head is straight with aligned capitulum and tuberculum. Below the capitulum and in the ventral margin of the rib head, are observed a shallow concavity and a deep slender concavity. Posteriorly the rib head is covered by ventromedially-to-laterodorsally oriented striations. Ventral to the tuberculum, on the anterior surface of the rib head is observed an oval rugose surface and probably represents the insertion of the *lig. costotransversarium*. The tuberculum is dorsally projected, squared in contour and separated from the capitulum by a deep concavity. The tuberculum shows a round but flat articular surface. Below the tuberculum it is observed a big and subtriangular pneumatopore. From the medial side of the tuberculum, rises a strong, dorsally projected and rugose ridge, which projects ventromedially reaching the posterior surface of the rib head. Furthermore, the lateral side of the tuberculum shows a rugose and laterally projected bump. Both structures (ridge and bump), represents the insertions of the *lig. costotransversarium*³⁹. On its posterior surface, the tuberculum shows a raised surface delimited by a round lip and enclosing numerous small foramina (probably of pneumatic origin). The capitulum is dorsomedially facing and shows an expanded and rugose articular surface for the parapophysis. The articular surface of the capitulum is oval in contour (mediolaterally wider than anteroposteriorly long) and saddle-shaped (laterally concave and medially convex). Immediately lateral to the capitulum is observed a short ridge surrounded by striations. This area corresponds to the attachment of the *lig. costovertebrale*³⁹. Finally, a set of rugosities is observed surrounding the articular surface of the capitulum as a ring, which probably constitutes the insertion of the *lig. costovertebrale*³⁹. Anteriorly, the capitulum shows two sets of striations: one of weak and oblique striations placed laterally to the

capitulum and one of almost horizontal and strong striations placed below the capitulum. Both sets of lineations are considered as the insertion of the *lig. costovertebrale*³⁹. In anterior view, from the shaft of the rib rises the anterolateral flange, which is deep and runs along the lateral margin of the shaft. On the medial side of the shaft, it is observed the anteromedial flange; which is sharp but weaker than the anterolateral one. Both flanges delimit an anterior concavity and, contrarily to the posterior side, do not intersect each other. Adjacent to the tuberculum and in the posterior face of the rib, it is observed the posterolateral flange which runs along the lateral margin of the bone and following its shaft. This flange is very deep and delimits a posterior concave surface. The preserved part of the rib is “8”-shaped in cross-section.

A fragmentary rib is identified as the left **sixth dorsal** mainly because of its big size (Fig. 11 G-I). It is only represented by an incomplete proximal part of shaft. It is notably stout, much more than other ribs. Its proximalmost preserved part shows a “T” shaped cross-section, with concave anterior and posterior margins. The anterior surface is deeper than the posterior one. Ventrally, the shaft becomes strongly thickened forming a hyperostosed “belly”. This belly is posteromedially projected and is thicker at mid-height. Posteriorly, it shows a deep and ovoidal pneumatopore that communicates with a big internal pneumatic chamber and with the posterior concave surface. The surface of the belly is covered with striations and rugosities. A low but stout posterolateral flange runs along the entire length of the rib.

Gastralia:

The total number of gastral ribs in *Maip* is unknown. The reconstructed transversal width of the largest and most completely preserved medial gastral rib was about 45 cm., with an estimated total length of 60 cm. The total width of the gastral complex (four articulated elements: two medial and two lateral ones) is estimated at about 120 cm. The widest point of the thorax of *Maip* (at the level of D6) would have had 140 cm. in transverse width.

Medial elements: These elements are dorsally curved with a thin shaft and a paddle-shaped medial end (Fig. 12 A-D). The anterior medial elements show a stouter and less anteroposteriorly curved shafts. The shaft becomes thinner towards its lateral end. In cross-section, the shaft is subcircular or ovoidal at mid-length and becomes subquadrangular towards the lateral end. Towards the medial end, the shaft becomes thinner because of the presence of a medial paddle that constitutes the surface for articulation with the opposite medial gastral element. Anteriorly, the shaft shows the articular surface for the lateral gastral element, which is represented by a concave or flat surface that may reach a fifth of the entire total length of the element. The paddle-shaped medial end shows an anterior flange that is anterodorsally projected and a posterior one that is posteroventrally oriented. This results in that the medial end of the element is posterodorsally facing. This posterodorsal surface articulates with the anteroventral surface of the posterior gastralia, resulting in the typical theropod interwoven gastral arrangement^{43,45}.

Lateral elements: These elements are rod-like and almost straight (Fig. 12 E-F). The longer preserved element reaches 30 cm. The shaft is oval in cross-section and exhibits its widest point close to the lateral

end. Its medial end is relatively thin and shows a concave articular surface with the medial gastral element that is exposed in posterior view. This surface does not reach half of the total length of the element. The lateral end of the element is relatively stout and ends in a rounded surface.

Shoulder girdle

Coracoid: The left coracoid is almost completely preserved, only lacking its dorsal margin and the biceps tubercle (Fig. 13). This bone is very thin with exception of its posterior that shows a strong buttress that was continuous with the scapula. In lateral view the coracoid is ovoidal in contour, being more than twice dorsoventrally tall than anteroposteriorly long. The lateral surface is nearly smooth and concave. Medially, the coracoid is deeply concave, this concavity being much deeper at its center. The scapulocoracoid suture is rugose.

The anterior margin of the bone is convex and shows a prominent anterior projection, which is absent in remaining megaraptorans (such as *Fukuiraptor*, *Megaraptor* or *Aerosteon*). Dorsal to this projection, the anterior margin shows rugosities for muscular attachment, and ventrally it shows a posteromedially facing articular surface. This surface appears to be absent in other megaraptorans such as *Fukuiraptor*, *Aerosteon* and *Megaraptor*. Based on its position it is possible to infer that it constituted the articular surface for the sternum. No single sternum has been recovered on megaraptorans, and it is not improbable that it was almost cartilaginous or poorly ossified.

Only the base of the bicep tubercle was preserved, but it seems to be robust and not reduced as in *Aerosteon*³³. The coracoid foramen is big, ovoidal and subvertically oriented. Posteriorly to the foramen, there are strong anteroposteriorly oriented striations that represent the anchoring of the *m. biceps brevis*⁴⁶. In medial view, the coracoid foramen is ovoidal, posteriorly oriented and close to the limit with the articulation with the scapula. It does not form a groove connecting with the scapula as is observed in *Aerosteon*¹⁴. The glenoid is straight and do not project laterally in a lip. The posteroventral process is prominent, subtriangular in contour when viewed from the side, and ventrally projected. It shows on its medial side, strong and curved rugosities that are subparallel to the margins of such process. Such structures are the attachment of the *m coracobrachialis*⁴⁶. *Maip* shows a relatively simple posteroventral process that lacks a vertical lamina, subglenoid ridge and a deep subglenoid fossa present in *Aerosteon*¹⁴. A subglenoid fossa is very shallow and poorly defined in *Maip*.

Discussion

The costovertebral ligaments in *Maip* and respiration in early tetanurans. As commented in the description, many vertebrae and ribs of *Maip* show striations or rugosities which should be interpreted as the attachment sites for the costovertebral and costotransversarium ligaments (Fig. 14). This condition is not commonly observed in other theropods, and thus, *Maip* offers the rare opportunity to discuss about the costovertebral ligaments of theropods. In most aspects, these attachments for the costovertebral ligaments resembles the condition previously described for vertebrae and ribs of tyrannosaurids⁴¹.

In *Maip* vertebrae and ribs exhibit striations surrounding the tip of the transverse process of dorsal vertebrae which are interpreted as the insertion site of the *lig. costotransversarium*.

In most amniotans, the *lig. costovertebrale* is composed by a fibrous membrane wraps the tip of the transverse process of vertebrae and the tubercle of the ribs as a sleeve-like structure and two main thickenings (one dorsal and one ventral) that bears all the weight of the bone³⁹. These thickenings are stronger parts of the ligament which by supporting all the weight leave strong marks in the bone³⁹. In tyrannosaurids, the anterior and posterior sides of the tip of the transverse process, as well as its dorsal surface show strong transversal striations, and a raised projection surrounded by concavities and ridges on its ventral side evidence the presence of the *lig. costotransversarium*³⁹. In tyrannosaurids, the insertion of this ligament is inferred by the presence of transverse striations on the anterior and posterior surfaces of the ribs tubercle, a raised and obliquely oriented ridge medial to the tubercle, and a rugose bump-like projection on the lateral margin of the rib³⁹. In *Maip*, the transverse processes of D3, D6 and D7 exhibit smooth longitudinal striations at the anterior and posterior faces, as well as strong longitudinal striations on its dorsal surface, which correspond to the fibrous membrane (Fig. 14, A1). The transverse processes show rugosities closer to its tip (Fig. 14, A1) and a raised rugose projection immediately ventral to the diapophyses (Fig. 14A2); the first one is referred to be the dorsal part of the *lig. costotransversarium* and the last one to be its ventral part. Similarly, the tubercle of DR1, DR2 and other indeterminate proximal ribs, shows striations along its anterior and posterior surfaces, which correspond to the fibrous membrane; an obliquely and rugose ridge at the medial side of the tubercle, represents the insertion of the dorsal part of the *lig. costotransversarium* and a round, raised and rugose bump laterally to the tubercle, corresponds to its ventral part (Fig. 14A3). This suggests that, as in tyrannosaurids and birds³⁹, the costovertebral joint of *Maip* was covered by a fibrous membrane, and that the *lig. costotransversarium* has two main parts placed at the dorsal and ventral parts of the joint between transverse processes and rib tubercles. ³⁹ noted that this condition is related with a kinetic joint between vertebrae and rib.

Regarding costovertebral ligaments, its anchoring is evidenced on the vertebrae and ribs of extant birds by means of scars surrounding the vertebral parapophyses and rib capitulum³⁹. In *Maip*, some vertebrae (axis, D2, D4-D6 and D9) show strong rugosities surrounding the parapophyses (Fig. 14A4-5). In D4 such rugosities are placed anteroventral to the parapophyses, forming a crescent-shaped surface, probably being the ventral part of the *lig. costovertebrale* (Fig. 14A4). In the axis, D2, D5-D6 and D9 the rugosities are observed dorsally as a thin and anteroposterior long area and probably represent the anchoring of the dorsal part of the ligament (Fig. 14A5). The capitulum of DR1-2 as well as other indeterminate elements shows obliquely oriented striations on its posterior surface, which could represent the fibrous membrane of the joint. Along the ventral surface of the capitulum there is a concave area with strong distal striations and small proximal rugosities; at the dorsal surface of the capitulum there exists a subtriangular area with a raised ridge and smooth rugosities, which corresponds to the dorsal part of the ligament (Fig. 14A3). In contrast to the *lig. costotransversarium*, the scars for the *lig. costovertebrale* are less clearly defined, however, based on preserved scars this ligament probably had dorsal and a ventral attachment sites.

When ribs and corresponding vertebrae of *Maip* are articulated together, the four sets of striae (two per ligament) become aligned in an obliquely oriented main axis. This may allow rib rotation when the animal was alive, and therefore, it was able to expand or contract the thoracic cavity during respiration. This condition constitutes a ventilation system that resembles that of birds, and is different from the respiratory system of other reptiles, such as those of crocodylians^{22,39,47}. This kind of respiration is correlated with some other morphological traits present in most tetanuran theropods, including *Maip*, such as the presence of long and upturned transverse process of dorsal vertebrae, lateroventrally oriented diapophyses and long and curved dorsal ribs with long and well-separated capitulum and tubercles^{39,47}.

It is possible that the systems of ligament related to an advanced pulmonary respiration was widespread among tetanurans. However, because striations surrounding transverse processes of dorsal vertebrae and ribs capitulum and tuberculum are very subtle, they may be easily eroded and/or unobserved, and thus, their absence may be probably regarded as an artifact.

The Campanian through Maastrichtian megaraptorid record from southern Patagonia. With the aim of inforce, the condition of new taxa of *Maip*, this specimen was compared with other contemporaneous megaraptorans records of some geological units of the southern part of Patagonia.

From Chorrillo Formation, *Maip* is not the unique record for this family for the Upper-most part of the Cretaceous but certainly, until now, it is the most complete. In addition to *Maip*, the Chorrillo Formation has yielded at least four more different records of Megaraptoridae: an isolated dorsal centrum (MPM 21546), an isolated tooth (MACN-Pv 19066) and two sets of associated teeth (MPM-PV-22864-5;^{3,38}). Posterior comparisons of the isolated dorsal centrum (MPM 21546) with unenlagiids such as *Unenlagia* shows that this bone probably pertains to this clade of theropods more than to megaraptorids (Motta and Aranciaga Rolando *pers. obs.*,⁴⁸).

Recovered teeth (MACN-Pv 19066, MPM-PV-22864-5) Chorrillo Formation of exhibits a similar size and morphology to those of mid- to big-sized megaraptorids (such as *Murusraptor*, *Orkoraptor*, and *Megaraptor*). MPM-PV-22864 and MPM-PV-22865 are almost identical in morphology differing, as expected, in those traits that vary within the anterior and posterior parts of the jaw (such as the symmetry or not of the tooth crowns). On the other side, tooth MACN-Pv 19066 differs from the remaining ones in the presence of a major number of distal denticles (5 per mm vs 3 per mm in all other megaraptorids;^{3,39}). Notwithstanding, MACN-Pv 19066 was collected in the area in 1980 but lacks specific stratigraphic and geographic provenances³.

In sum, *Maip* is the more complete, by far, megaraptorid from Chorrillo Formation and the only with enough diagnostic anatomical traits and stratigraphic control to be considered new taxa.

Within other Campanian through Maastrichtian units from Patagonia, another unity which yielded megaraptorid remains is Lago Colhué Huapi Formation, in Central Patagonia (Chubut Province;^{20,35,36,49}). These records are: two isolated unguals (UNPSJBPV 1028 and UNPSJB-PV 1102;^{35,36}), an associated

manual ungual I and metatarsal III (UNPSJB-PV 1046 and UNPSJB-PV 1066;^{35,36}), and a yet-undescribed skeleton (UNPSJB-PV 1104;⁴⁹). Except for the latter specimen, the size of which is unknown, all these records represent mid- to big-sized megaraptorids (more than 6 meters long;⁵⁰). Nevertheless, the isolated nature of the specimens makes impossible estimate the age or the size of the specimens, and thus, do not allows us to find differences or similarities with *Maip*.

The Cerro Fortaleza Formation underlies the Chorillo beds, and is often referred as to Campanian-Maastrichtian in age. This unit has yielded the mid-sized megaraptorid *Orkoraptor* (6 meters long;³⁴). *Maip* differs from *Orkoraptor* by the absence, on its mid-caudal vertebrae, of deep prezygapophyseal-centrodiapophyseal fossa, horizontally disposed pre- and postzygapophyses, anteroposteriorly long hypantrum, and strong and stout transverse process. For these reasons, *Maip* and *Orkoraptor* and interpreted as different taxa based on the size of their respective holotypes and the morphology of its caudal vertebrae.

In sum, until now, *Maip* not only is the second taxa to be nominated in the southern part of Patagonia but also the most complete megaraptorid skeleton by far, the biggest species and the youngest record.

Maip compared with other megaraptorid and non-megaraptorid theropods. Besides that, *Maip* is the youngest and biggest megaraptorid record, its skeleton is one of the most complete. For this reason, this taxon was compared with other megaraptorids from Patagonia as well as other tetanurans with the aim to find new anatomical information.

The main difference between *Maip* and all other megaraptorids is its major size. In this sense when compared with *Aerosteon* (the second megaraptorid in size), the vertebrae of *Maip* are slightly bigger but also notably stouter or bulkier.

The axis of *Maip* is anteroposteriorly narrow and dorsoventrally tall. Besides the axis of *Maip*, the other known axis from Megaraptoridae is that of the juvenile of *Megaraptor* (MUCPv-595;¹⁰). Compared with *Maip*, the axis of *Megaraptor* is much anteroposteriorly longer and dorsoventrally lower and the postzygapophyses and the neural spine are much transversally wider. Moreover, the morphology observed in *Megaraptor* resembles more to the condition of most theropods (such as *Allosaurus* or *Sinraptor*;^{42,44}) than with *Maip*. Within Theropoda, the proportions of the axis of *Maip* resembles more to tyrannosaurids (such as *Tyrannosaurus*;⁴³) and carcharodontosaurids (such as *Acrocanthosaurus*), which have anteroposteriorly short axis. The high/width ratio of the axis is 2.1 times in *Maip* and *Tyrannosaurus*, 1.8 in *Acrocanthosaurus* and 1.3 in *Allosaurus*. The intercentrum of *Maip* is notably ventrally placed being slightly posterior to the parapophyses. This contrasts to the observed in most theropods where such structure is observed anteriorly to the pleurocentrum of the axis. Regrettably, the axis of the juvenile specimen of *Megaraptor* do not preserves the intercentrum¹⁰ and, thus, the condition of *Maip* is unique of this taxon. The neural spine of the axis of *Maip* lacks a transversally wide spine table as the observed in tyrannosaurids^{43,50}. Nevertheless, the neural spine of *Maip* is notably low, being slightly lower than those of *Allosaurus* or *Tyrannosaurus* but much lower when compared with

carcharodontosaurids (such as *Acrocanthosaurus* or *Concavenator*,^{51,52}). In *Maip* the postzygapophyses are round being slightly transversally wider than anteroposteriorly long, which seems the condition for *Tyrannosaurus*⁴³. In contrast, allosauroids such as *Allosaurus* and carcharodontosaurids (such as *Acrocanthosaurus* and *Giganotosaurus*) shows large postzygapophyses that are notably transversally wider than long. Furthermore, the orientation of the articular surface of the postzygapophyses is subhorizontal or slightly upturned in *Maip* and other theropods such as *Allosaurus* or *Tyrannosaurus*. In contrast, in carcharodontosaurids the articular surface of the postzygapophyses are strongly dorsally oriented. The epipophyses of *Maip* are moderate as occurs in many tetanurans⁵³, however, in carcharodontosaurids, the epipophyses are notably developed and strongly dorsolaterally projected. In sum, the axis of *Maip* shows a unique morphology which could be autapomorphic of this species or common to its group, until new megaraptorid skeletons come to light this cannot be confirmed. Finally, contrarily to the proposed by some previous phylogenetic analyses^{1,15} the axis of *Maip* shows substantial differences with carcharodontosaurids.

The D2 of *Maip* resembles in morphology of comparable vertebrae of *Murusraptor* and *Aerosteon*. However, proportionally *Maip* and *Aerosteon* are much stouter than *Murusraptor*. Alike, the neural arch of the D2 of *Maip* is much stouter and dorsoventrally lower than those of *Allosaurus*, *Sinraptor* and *Concavenator*^{42,44,52}. On the other side, larger theropod species like *Tyrannosaurus* or *Giganotosaurus* and *Mapusaurus* shows stout columns that resembles more to the observed in large-sized megaraptorans. Furthermore, the articular surface of the prezygapophyses of anterior dorsal vertebrae of *Maip* and *Aerosteon* are round, stouter and more anteriorly projected than those of *Murusraptor*. Interestingly, the prezygapophyses of *Maip* are placed below in the neural arch and do not reach the base of transverse process and the base of the neural spine. This condition is shared with the D4 of *Aerosteon* and the first dorsal vertebrae of derived tyrannosaurids^{14,43}. In contrast, the prezygapophyses surpass the dorsal margin of the base of the transverse process in D3 of the mid-sized megaraptorid *Murusraptor*, and the D2 of small-sized tyrannosauroids (such as *Guanlong*), as well as most tetanurans such as *Allosaurus*, *Sinraptor*, *Lajasvenator* and *Neovenator*. In sum, the dorsal vertebrae of *Maip* shares some conditions that are only observed in very large theropod species which suggests that this could be size-dependent traits.

In the mid-dorsals of megaraptorids (such as the D6 and D9 of *Maip*, the D7 of *Murusraptor*, the D8 of *Aerosteon* and the articulated column of the juvenile of *Megaraptor*) the transverse process is dorsally directed (or slightly posterodorsally) but not as in most theropods (such as *Allosaurus*, *Tyrannosaurus* or carcharodontosaurids) where the transverse processes are strongly posterodorsally projected. This unique condition of megaraptorids is directly related with a more lateral position of the anterior and posterior centrodiapophyseal lamina (in most theropods, these are posterolateral oriented giving the posterior projection of the transverse process) and the minor size of the prezygapophyseal-centrodiapophyseal fossa. In sum, all megaraptorids share the presence of less posteriorly oriented transverse process in mid-dorsal vertebrae.

The proximal caudal vertebrae of *Maip* shows tall neural spines. This condition is shared with other megaraptorids (such as *Megaraptor* or *Murusraptor*) as well as tyrannosaurids and *Allosaurus*. On the contrary, carcharodontosaurids shows strongly taller proximal caudal neural spines⁵². In addition, the height/anteroposterior width ration of the proximal caudal of megaraptorids, tyrannosaurids and *Allosaurus* is less than 2, while in carcharodontosaurids (such as *Mapusaurus* and *Concavenator*) the same ratio is between 2 and 4.

The coracoid only complete coracoid known for Megaraptoridae rather than *Maip* is that of *Aerosteon*. *Maip* resembles *Aerosteon* in having a strongly projected ventral process and a deep posteroventral fossa¹⁴. Notwithstanding, in the description was noted that *Maip* exhibits a simpler posteroventral cavity than *Aerosteon*, which results in an autapomorphic character of the former taxa. Furthermore, in *Maip* the coracoid is stouter and anteroposteriorly wider than *Aerosteon*, being the high/width ratio 1.6 in *Maip* and 2.0 in *Aerosteon*. In sum, the coracoid of *Maip* shows a unique anatomy and proportion, which reinforces its condition of new taxa.

Phylogenetic results. With the aim of testing the validity of *Maip* as well as its phylogenetic relationships with other theropods, two different phylogenetic analyses were performed (see Supplementary Information I). The analyses with and without fragmentary taxa show a topology similar to those of previous analyses^{19,12} being megaraptorans nested within Coelurosauria, and forming the sister group of Tyrannosauroida (Fig. 15A).

The analysis including all taxa results in 2560 most parsimonious trees (MPTs) of 1453 steps. Within Megaraptora, this analysis shows *Phuwiangvenator* as the basalmost member of the clade, and as the sister taxon of a polytomy including *Vayuraptor*, a indeterminated Australian megaraptorid (LRF 100-106), *Fukuiraptor*, *Aoniraptor*, *Australovenator*, the indeterminated Patagonian megaraptorid from Bajo Barreal Formation (UNPSJB-PV-944/958), *Megaraptor* and *Orkoraptor*. These theropods constitutes the sister group of the subclade including *Murusraptor*, *Aerosteon*, *Tratayenia* and *Maip*.

Aoniraptor results as a megaraptoran of uncertain affinities (Fig. 15A), like has been observed in other works^{13,31}. The enigmatic theropod *Gualicho*¹⁸, which in some analyses⁵⁴ has been considered as a possible synonym of *Aoniraptor*, here is deeply nested within Tyrannosauroida, very far from *Aoniraptor* (Fig. 15A-B). Furthermore, 17 extra steps are required to move *Gualicho* as the sister taxa to *Aoniraptor*. In sum, according to¹³, we conclude that both taxa are not closely related.

Regarding the indeterminated megaraptorid from Bajo Barreal Formation (UNPSJB-PV-944/958;²⁰), this specimen shares with other South American taxa a dorsal vertebral centrum which is anteroposteriorly longer than dorsoventrally tall (Ch. 106-1) and a manual ungual phalanges with a flexor tubercle that shows a wide lateromedial sulcus (Ch. 292-2). In spite of its fragmentary nature, UNPSJB-PV-944/958 is considered to be more closely related to South American forms than with those of other landmasses of Gondwana. Other isolated megaraptoran records from South America are those of the Campanian Uberaba Formation⁵⁵, the Maastrichtian Sao José do Rio Preto Formation⁵⁶, and Upper Cretaceous

sediments of Brazil³⁰, which remain as indeterminate megaraptorans because of their fragmentary nature.

The second analysis pruning fragmentary taxa with less than the 15% of the skeleton, results in 80 most parsimonious trees (MPTs) of 1455 steps (Fig. 15B). The Consistency Index (CI) is 0.312 and the Retention Index (RI) is 0.599. The tree topology is very similar with the first analysis but shows a higher resolution within Megaraptora. As in previous works, the more basal forms of this clade are the Asian *Phuwiangvenator*, *Vayuraptor*, and *Fukuiraptor*, which constitute successive sister taxa of Megaraptoridae^{2,7,10,12,19}. Among megaraptorids, the Australian LRF 100-106 and *Australovenator* represent the more basal members of the clade and are more closely related to each other than to South American megaraptorids (See Supplementary Information I). The latter include a clade with taxa from the early Late Cretaceous (*Megaraptor* and *Murusraptor*) are another clade formed by younger Patagonian megaraptorids (*Tratayenia*, *Orkoraptor*, *Aerosteon* and *Maip*). Regarding robustness values, Bremer support and bootstrap frequencies (absolute and GC) are relatively low (as in all previous phylogenetic analyses of this clade) and are slightly higher in the analysis when fragmentary taxa are excluded (Fig. 15; Supplementary information I).

Recovering two clades of South American megaraptorids. One of the more outstanding results of the present analysis (Fig. 15B) is the recovering of two new clades (the first including the second one) comprising some derived megaraptorids from South America. The more inclusive clade (Clade “A”) comprises *Megaraptor*, *Murusraptor* and the less inclusive clade (Clade “B”). This latter includes *Orkoraptor*, *Tratayenia*, *Aerosteon* and *Maip*.

The Clade “A” is supported by three synapomorphies (see SI): 1) Absence of mesial denticles (Ch. 2-2; Fig. 16A): such denticles are observed in *Fukuiraptor*, *Australovenator* and the isolated megaraptoran tooth from Strzelecki Group of Australia²², but they are absent in *Megaraptor*, *Murusraptor*, *Orkoraptor* and the megaraptorid tooth from Chorrillo Formation (MACN-Pv 19066). 2) Tibia, dorsally curved in lateral view (Ch. 355-0; Fig. 16B) which is observed in *Murusraptor*, *Aerosteon* and *Orkoraptor* but it is absent in *Australovenator*. 3) Manual ungual phalanges with flexor tubercle with a wide lateromedial and smooth platform (Ch. 292-2; Fig. 16C). This trait is absent (state 0) outside Megaraptora as well as on its basal forms such as *Fukuiraptor*, the Thai taxa and the fragmentary ungual of Strzelecki Group (NMV P186153;²²); instead, the Australian *Australovenator*, LRF 100/106 and the Megaraptoridae cf. *Australovenator wintonensis* [NMV P239464;²³] shows a lateromedial sulcus (state 1). In contrast, in *Megaraptor*, the megaraptorids from Bajo Barreal Formation (UNPSJB-PV 944;⁵⁰) and Lago Colhué Huapi Formation (UNPSJB-PV 1102 and 1046;^{35,36}) and the referred ungual from *Aerosteon*³³ exhibits a wide lateromedial platform (state 2).

The Clade “B” (including *Maip*, *Aerosteon*, *Orkoraptor* and *Tratayenia*) is supported by two synapomorphies (See SI): 1) Dorsal vertebrae with a bifurcated lamina anterior to the transverse process and forming an accessory fossa (Ch. 352-1; Fig. 16D). This is observed in all the dorsal vertebrae of *Maip*, *Tratayenia* and *Aerosteon* while the megaraptorid from Bajo Barreal Formation (UNPSJB-PV-944/958),

Murusraptor and *Megaraptor* lacks this accessory fossa and lamina. 2) Round and big articular facets of pre- and postzygapophyses of proximal caudal vertebrae (Ch. 353-0; Fig. 16E). This condition is observed in the caudal vertebrae of *Maip*, *Orkoraptor* and *Aerosteon* while *Megaraptor*, *Aoniraptor* and *Murusraptor* shows subtler and thin prezygapophyses in proximal caudal vertebrae.

Interestingly, Clade “A” gathers most of the forms of Patagonia after the Cenomanian-Turonian limit. Further, all these forms surpass the 6 or 7 meters long. This information supports Lamanna *et al.*⁵⁷, who hypothesized that megaraptorids underwent a trend in body size increase during the Upper Cretaceous in South America. Moreover, Clade “B” gathers Santonian through Maastrichtian megaraptorids from South America, which also, constitute the bigger forms of Megaraptora (between 8 and 10 meters long;^{32,33,55,56}). These new clades reinforce the proposed by Lamanna *et al.*⁵⁷, showing a diversification and a directly proportional size increase during the Upper Cretaceous of Patagonia.

Other potential characters for the South American megaraptorids. In the present analyses were found some other potential traits which because of the poor overlapping of bones within Megaraptora cannot be considered as true apomorphic traits. Nevertheless, were included here for future analyses. One of these characters is the presence of dorsal centrum anteroposteriorly longer than tall (Ch. 106-1; Fig. 17A), condition that it is shared by *Megaraptor*, *Murusraptor*, *Tratayenia*, *Maip*, *Aerosteon* and the indeterminate megaraptorid from Bajo Barreal Formation (UNPSJB-PV-944/958; described in Lamanna *et al.*⁵⁷ as a caudal element, but here reinterpreted as a dorsal centrum). In contrast, the dorsal centra are longer than tall in *Fukuiraptor*, *Phuwiangvenator* and the isolated dorsal centrum of Strzelecki Group in Australia (NMV P221187;²²).

Another two potential features are: presence of two transverse grooves on the anterior surface of the astragalar body, and ascending process not reaching the entire width of the astragalar body and with a medial “step” in anterior view (Fig. 17B). These features are observed in *Fukuiraptor*, *Vayuraptor*, *Phuwiangvenator*, *Australovenator*, Megaraptoridae cf. *Australovenator wintonensis*, from Eumeralla Formation (NMV P253701;²³) and an isolated astragalus from Strzelecki Group (NMV P150070;²²). In contrast, the astragalus of *Aerosteon* shows only one groove at the base of the ascending process and the ascending process occupies all the width of the astragalar body and does forms a “step” in anterior view.

On the other side, *Rapator ornitholestoides* and *Australovenator*^{8,58} shows a metacarpal I with a strongly proximally projected lateroventral process, a posteroventral process notably more proximally projected than the rest of the bone and distal articular hemicondyles subequal in size (Fig. 17C). All these features contrast with *Megaraptor*⁷ which lacks a lateroventral process, its posteromedial process does not surpass proximally the rest of the bone and the lateral hemicondyle is notably bigger than the medial one. Moreover, the available ulnae of Australia (NMV P186076, LRF 100/106 and *Australovenator*,^{8,22,24}) shares the presence of a lateral tuberosity laterodorsally projected in proximal view (Fig. 17D). This feature contrasts with *Megaraptor*^{6,7} that exhibits a laterally projected lateral tuberosity on its ulna.

Regrettably, the Australian record is very fragmentary to make further statements. Notwithstanding, the anatomical information afforded by *Maip* reveals that there is two different megaraptoran faunas within Australia (See Supplementary Information I).

In sum, with the available record of Megaraptora until more complete skeleton comes to light we cannot precise more the taxonomic or phylogenetic status of such traits.

The diversification of Megaraptora in South America. Lamanna et al.⁵⁷ noted that within South America, megaraptorids exhibits a size increase and a taxonomic diversification in the upper part of the Cretaceous. Our analysis supports this and also, based on our phylogenetic results, we observe a correlation between the morphology, size and age in the megaraptoran records (Fig. 18A-C). The smaller (between 4-4.5 meters) and basal megaraptoran species are observed in the Barremian-Aptian sediments of Asia, South America and Australia^{4,5,11,21,22}. The mid-sized (between 4,5-6 meters) megaraptorid forms are present in Aptian-Lower Turonian of Australia and South America^{20,22,24,26,27,31}. In Turonian-Conician times, the megaraptorids are only documented in South America, with medium to large-sized (between 6-7 meters) forms, more closely related each other than with other members of the group. Finally, from Santonian to Maastrichtian times, this endemic clade of South American megaraptorids becomes bigger (between 7-10 meters). This tendency, previously noted by *Lamanna et al.*⁵⁷, is supported by our phylogenetic results, which shows that largest megaraptorids are nested in the crown-group.

During Turonian-Conician times the records of Megaraptoridae become notably more numerous in South America, suggesting a diversification for the group (Fig. 18B), but also, that megaraptorids occupied a more important role in the Upper Cretaceous ecosystems of South America (see below).

Furthermore, the pneumaticity within Megaraptora becomes progressively more developed through more derived forms. This could be related with a major necessity of reducing the metabolic cost of the skeleton in bigger forms^{59,60} and, for this reason, related with the size-increase of the group. However, until now, we cannot quantify the pneumatic condition of theropods and further analyses are necessary.

In sum, we hypothesize support the exposed by Lamanna *et al.*⁵⁷ that megaraptorids becomes progressively bigger and much more numerous during all the Cretaceous. Furthermore, we find that within South America, after the Cenomanian-Turonian limit these theropods experimented a more abrupt increase (Fig. 18A-C). Noteworthy, after the Cenomanian, occur the extinction of carcharodontosaurids and spinosaurids, the apex predator until that moment in the Southern landmasses^{2,40,61}.

The predators of Patagonia after the extinction of Carcharodontosaurids. Several authors have proposed that an extinction event during the Cenomanian-Turonian interval may affect many vertebrate groups in both hemispheres^{39,40,62}. Authors discuss the impact of this event or if this extinction represented a single event or successive processes separated by million years⁶¹. Nevertheless, there is consensus that after Cenomanian-Turonian time interval many dinosaurian groups become extinct in tandem with the origin and diversification and numerical abundance of others^{2,39,40,61-64}. Here, we discuss the

replacement of predators after this period of time in the Southern continents comparing it with those of the North hemisphere.

For the Northern Hemisphere, several authors proposed an ecological replacement during the Cenomanian-Turonian limit^{16,63,64}. For this interval, carcharodontosaurids (or allosauroids) and tyrannosaurids coexisted, being tyrannosaurids small forms occupying the role of small- to mid-sized predators, and carcharodontosaurids being larger species and the top predators of that ecosystems. This change in the Cenomanian-Turonian limit, when carcharodontosaurids becomes extinct and tyrannosaurids underwent a notable diversification involving a higher number of taxa alongside with a sustained increase in body size, thus occupying the role of apex predators^{16,63,64}. Recently, Holtz⁶⁵ proposed that big- and middle-sized niches in the carnivorous guilds of Upper Cretaceous of Laramidia and Asia have been dominated by adults, subadults and juvenile of tyrannosaurid species. During the ontogeny, juvenile specimens of different tyrannosaurid species occupied distinct niches from their adult forms. The dominance of tyrannosaurids could have restricted the carnivorous diversity of Northern landmasses to small-size paravians such as troodontids, dromaeosaurids and microraptorans⁶⁵.

As for the Southern landmasses refers, several different carnivorous dinosaurs are recorded in Upper Cretaceous formations, including abelisaurids, carcharodontosaurids, megaraptorids and paravians, but the record of these clades shows changes along the time. Many authors have noted the extinction of carcharodontosaurids after Cenomanian times^{2,39,40,61,66} and some have suggested its replacement by other theropods groups which became common in Patagonia in post-Cenomanian times, such as abelisauroids, unenlagiids, and megaraptorids^{40,61}. Our phylogenetic analysis shows that megaraptorans were present in South America previous to Cenomanian-Turonian times as mid-sized predators (SMNS 58023 and *Aoniraptor*,^{11,31} but, after this time, megaraptorids expanded and diversified resulting in a major body size and a higher number of taxa (Figure 18D; Supplementary Information III). This also can be observed simply looking the size of the taxa before and after of the extinction, the pre-extinction members are smaller (5-6 meters) than the post-extinction one (6-10 meters). In this sense, megaraptorids trend to become progressively bigger since its basalmost forms but this trend exhibits an abrupt increase after the Cenomanian-Turonian limit. We hypothesize that the lack of big-size predators after the Cenomanian-Turonian extinction (including carcharodontosaurids, spinosaurids and big-sized abelisaurids) probably allowed megaraptorids to diversified and occupy the “empty” niche of top predators in South America, in a way similar to the pattern described above for tyrannosaurids in the Northern Hemisphere.

The family Abelisauridae was widespread along South America, Africa, Madagascar and Europe from the Albian (*Genusaurus* is considered an abelisaurid) to Maastrichtian times. Along the evolutionary history of abelisaurids, their size range do not increase in a lineal way as it does in megaraptorids, notwithstanding, a general pattern can be recognized (Fig. 18D). The basalmost forms of the family are known from the Cenomanian (and Albian with *Genusaurus*) times and represent small- to large-sized forms between 4 (or 3 considering *Genusaurus*) and 7 meters long^{45,67} (Fig. 18D). This size range

previous to the extinction shows a small increment with some species like *Ekrixinatosaurus* or *Skorpiovenator*. This wide range of sizes reduces after the Cenomanian-Turonian interval where the taxa exhibit between 3.5-5 meters long in the Turonian-Conician. Then, the average size of its members gradually starts to grow from the Santonian to Campanian times, when Abelisauridae shows sizes between 5 and 7 meters⁴⁵. Finally, in the Maastrichtian are observed the most derived members of the family which shows sizes ranging from 4,5 through 9 meters long^{14,45,67}. As commented above, the size of abelisaurids is diverse and sometimes coexist small and large-size forms⁴⁵. Nevertheless, after the Cenomanian-Turonian extinction of carcharodontosaurids and spinosaurids (as well as many other vertebrate groups), some pattern of diversification can be observed in the families of Southern predators. In this sense, the size of abelisaurids after extinction of Cenomanian-Turonian is small (3-6 meters), when it is compared with pre-extinction members (5-8 meters). This suggests that the extinction event also hits abelisaurids, but the big-sized forms are much more affected than the smaller ones (which are documented after the extinction). Furthermore, Big-size abelisaurids species with 6-7 meters long are founded again in beds of the end of Cretaceous (Fig. 18).

Paravians represent one of the most interesting cases of increase of body size within the theropods from Southern continents, which is probably related to the Cenomanian-Turonian extinction. (Fig. 18D). Paraves usually include species that not surpass the 2 meters long and the big-sized forms within this clade are scarce⁶⁸⁻⁷⁰. The oldest paravians found in southern continents are restricted to Cenomanian and Turonian beds of Patagonia and include the small-sized paravians *Buitreraptor* and *Overoraptor* from Candeleros (Cenomanian) and Huincul (Cenomanian-Turonian) Formations, respectively^{71,72}. Both taxa show 1.5 meters of body length. Nevertheless, after the Turonian limit, the record of paravians in the Southern continents increases. For the Conician, unenlagiids are represented by numerous records of small- and small-to-mid-sized specimens (such as *U. comahuensis*, *U. paynemili*, *Neuquenraptor* and *Pamparaptor*,^{73,74}). For the uppermost Cretaceous period, the record of unenlagiids comprises small- and big-sized form such as *Austroraptor*, *Imperobator*, and two indetermined paravians from Africa and Patagonia^{3,69,75,76}. This suggest that as occurs with abelisaurids and megaraptorids, the paravian record in Patagonia with major body length are observed after the Turonian limit. Furthermore, *Austroraptor*, which exhibits 5 meters long, is one of the biggest records of paravians along with its northern (but pre-Maastrichtian) relatives: *Achillobator*, *Dakotaraptor*, and *Utahraptor*⁶⁹. The record of paravians in South America suggest that, after the Turonian limit, this clade exhibits an increase of the body length reaching extreme sizes as the case of *Austroraptor* and occupying a top predator role.

In sum, we observe that megaraptorids, abelisaurids and unenlagiids show an increase of the body length after the Cenomanian-Turonian limits and, for South America, we relate this with the extinction of carcharodontosaurids (Fig. 18D). We hypothesize that these groups share the role of apex predators within the Southern continents on the Upper Cretaceous. The role of top-predator in continental environments of South America was occupied by at least two theropod clades, including Megaraptora and Abelisauridae. Further, this could be extended to the big-size paravian *Austroraptor* that is one of the

biggest theropod from its unit. In this way, South American big carnivorous dinosaurs are more diverse than in Laramidia and Asia, in with only tyrannosaurids were the dominant among big predators.

In summary, *Maip macrothorax* is the biggest and youngest megaraptorid record. *Maip* help to complete the poorly known skeleton of megaraptorids affording many unknown bones for the clade such as the axis, D2, D5, D6, D9, caudals, many cervical and thoracic ribs and gastral elements. Furthermore, the anatomical evidence afforded by *Maip* solve the internal relationships of Megaraptora, one of the most important enigmas in the phylogeny of megaraptorans. The results of the phylogenetically phylogenetical analysis show two new clades: the first to nest most of South American forms (clade “A”) and the second one that is less inclusive and only comprising the most derived forms of the first group (clade “B”). This results support previous analyses that suggests a trend to a size increment of the south American megaraptorid forms. In addition, our results provide evidence a diversification of megaraptorids within South America. Finally, the diversification and the size increment are correlated with role change after the extinction of carcharodontosaurids. Similarly, the register of abelisaurids and unenlagiids forms shows a body-size increment after the Cenomanian-Turonian extinction. This work suggests that, contrarily to Laramidia were carcharodontosaurids was replaced only by tyrannosaurids, in Gondwana the megaraptorids, abelisaurids and probably unenlagiids became the top predators of their ecosystems.

Methods

Description. Several bones were digitally scanned by surface scanning with a Shinning 3D Einscan Pro. The resulting .obj files were then rendered with 3D Slicer software and converted to image files. For description of the column, each vertebrae or rib were nominated with a “D” for dorsal, “Ca” for caudal, “CR” for cervical rib, “DR” for dorsal rib followed of the number of the bone.

Phylogenetic analyses. Two different phylogenetic analysis were performed: one with some fragmentary forms and one without such specimens (Supplementary Information 1A).

Analyses of theropod faunas of Patagonia. Spinosauridae are big-size theropods well recorded in Europe, Africa and Brazil^{77,78} which vanished at the end of the Cenomanian^{79,80}. The role of small sized theropods (less than 2 meters) was played by a variety of clades, including Noasauridae and Alvarezsaurids^{81–84}. Both groups never reach large sizes, all its specimens come from after the Cenomanian-Turonian limit and, for this reason, do not allow us to test the possible size increment through time and show poorly known ecological roles so, for all these reasons, was also excluded from this analysis^{85,86}.

Other theropods from Patagonia that are excluded from this analysis are *Bicentenaria argentina* (Candeleros Formation; Cenomanian;⁸⁷) and *Aniksosaurus darwini* (Bajo Barreal Formation; Cenomanian-Turonian;^{88,89}). Both represent poorly known theropods, with unresolved phylogenetic affinities (our analysis is based in families) and, in the case of *Anyksosaurus*, all specimens represent juvenile specimens.

Estimation of body-size of Megaraptora members as well as those of abelisaurids and unenlagiids, follows the analyses of Lamanna *et al.*⁵⁷ and Grillo and Delcourt⁸⁵ (See Supplementary information II). *Maip* was approximately nine to ten meters long, its body-length was estimated based on comparisons with the proportions of the vertebrae of *Aerosteon* and *Allosaurus* (Supplementary information III). The methodology of Grillo and Delcourt⁸⁵ was not applied because it relies on complete specimens to calculate an initial equation of body size (and from there extrapolate another equation for less complete specimens) and all megaraptoran specimens have been incompletely preserved.

Declarations

Author contributions:

A.M.A.R, M.J.M. excavated the fossil. A.M.A.R. prepared the materials. A.M.A.R., M.J.M., F.L.A. wrote the manuscript, drew the figure and conducted the phylogenetic analyses. M.M., and T.T. found the expedition and revised the manuscript. F.N. conducted the expedition and revised the manuscript.

Acknowledgements:

Thanks to the late Coleman Burke (New York), for his encouragement and financial assistance to carry on the first field explorations. Dr. Yoshihiro Hayashi, former Director General, National Museum of Nature & Science, Japan, for his support for the project by funding a major part of the expedition from the internal grant from the museum. Facundo Echeverría and his wife Daphne Fraser (La Anita farm) offered their valuable geographic knowledge of these territories, allowing us an easy access to fossil sites with our 4x4 vehicles. Special thanks to Federico Braun for allowing access to his property. Oscar Canto and Carla Almazán (Secretaría de Cultura) for supporting our projects and explorations in Santa Cruz. Also, we thanks to the family De Pasqua for allowing the preparation of the specimen in his house during quarantine, especially to Julieta De Pasqua who help during the preparation of the specimen. Many thanks to Santiago Miner for scanning all the bones and design some figure for the manuscript. Special thanks to Agustin Ozan who draw the reconstruction of this new species. Special thanks to the geologists F. Nullo, F. Varela, D. Moyano Paz, M. Coronel and E. Vera for their valuable comments on stratigraphy and regional geology at Santa Cruz province. Finally, thanks to S. Rozadilla, F. Brissón Eglí, G. Muñoz, M. Cerroni and members of the LACEV team for help during the extraction, preparation and writing the manuscript.

References

1. Benson, R. B., Carrano, M. T., & Brusatte, S. L. A new clade of archaic large-bodied predatory dinosaurs (Theropoda: Allosauroidae) that survived to the latest Mesozoic. *Sci. Nat.*, **97**(1), 71–78 (2010).

2. Novas, F. E., Ezcurra, M. D., Agnolin, F. L., Pol, D., Ortiz, R. New Patagonian Cretaceous theropod sheds light about the early radiation of Coelurosauria. *Rev Mus Argentino Cienc Nat.* **14**:57–81. doi:10.22179/REVMACN.14.372 (2013).
3. Novas, F., Agnolin, F., Rozadilla, S., Aranciaga-Rolando, A., Brissón-Egli, F., Motta, M., & Gentil, A. Paleontological discoveries in the Chorrillo formation (Upper Campanian-Lower Maastrichtian, Upper Cretaceous), Santa Cruz Province, Patagonia, Argentina. *Rev Mus Argentino Cienc Nat nueva serie.* **21** (2):217–293. doi:10.22179/REVMACN.21.655 (2013).
4. Samathi, A., Chanthasit, P., & Sander, P. M. Two new basal coelurosaurian theropod dinosaurs from the Lower Cretaceous Sao Khua formation of Thailand. *Acta Palaeontol Pol.* **64**(2):239–260. doi:10.4202/app.00540.2018 (2019).
5. Samathi, A., Suteethorn, S., Pradit, N., & Suteethorn, V. New material of *Phuwiangvenator yaemniyomi* (Dinosauria: Theropoda) from the type locality: implications for the early evolution of Megaraptora. *Cretac. Res.*, **105093** (2021).
6. Calvo, J. O., Porfiri, J. D., Veralli, C., Novas, F. E., & Poblete, F. Phylogenetic status of *Megaraptor namunhuaiquii* Novas based on a new specimen from Neuquén, Patagonia, Argentina. *Ameg.* **41**:565–575 (2004)
7. Novas, F. E., Aranciaga-Rolando, A. M., & Agnolín, F. L. Phylogenetic relationships of the Cretaceous Gondwanan theropods *Megaraptor* and *Australovenator*: the evidence afforded by their manual anatomy. *Mem Mus Vict.* **74**:49–61. doi:10.24199/j.mmv.2016.74.05 (2016)
8. White, M. A., Cook, A. G., Hocknull, S. A., Sloan, T., Sinapius, G. H., & Elliott, D. A. New forearm elements discovered of holotype specimen *Australovenator wintonensis* from Winton, Queensland, Australia. *PLoS One.* **7**(6):e39364. doi:10.1371/journal.pone.0039364. (2012).
9. White, M. A., Benson, R. B.J., Tischler, T.R., Hocknull, S.A., Cook, A.G., Barnes, D.G., Poropat, S.F., Wooldridge, S.J., Sloan, T., & Sinapius, G.H.K., et al. New hind limb elements pertaining to the holotype reveal the most complete Neovenatorid Leg. *PLoS One.* **8**(7):e68649. doi:10.1371/journal.pone.0068649 (2013a).
10. Porfiri, J. D., Novas, F. E., Calvo, J. O., Agnolín, F. L., Ezcurra, M. D., & Cerda, I. A. Juvenile specimen of *Megaraptor* (Dinosauria, Theropoda) sheds light about tyrannosauroid radiation. *Cret Res.* **51**:35–55. doi:10.1016/j.cretres.2014.04.007. (2014).
11. Aranciaga Rolando, A. M., Brissón Egli, F., Rozadilla, S., Novas, F. E.. Metatarsals from the upper cretaceous from Mendoza, Argentina. Resúmenes XXIX Jornadas Argentinas de Paleontología de Vertebrados. *Ameg.* **52**(4 (R), 1 - 42. Retrieved from <https://www.ameghiniana.org.ar/index.php/ameghiniana/article/view/2935> (2015)
12. Aranciaga Rolando, A. M., Novas, F. E., & Agnolín, F. L. A reanalysis of *Murusraptor barrosaensis* Coria & Currie (2016) affords new evidence about the phylogenetical relationships of Megaraptora. *Cretac. Res.* **99**, 104-127 (2019).
13. Aranciaga Rolando, A. M., Garcia Marsà, J., & Novas, F. Histology and pneumaticity of *Aoniraptor libertatem* (Dinosauria, Theropoda), an enigmatic mid-sized megaraptoran from Patagonia. *J. Anat.*

- 237**(4), 741–756 (2020).
14. Aranciaga Rolando, A. M., Méndez, A., Canale, J., & Novas, F. Osteology of *Aerosteon riocoloradensis* (Serenó et al. 2008) a large megaraptoran (Dinosauria: Theropoda) from the Upper Cretaceous of Argentina. *Hist. Biol.*, **1-57** (2021).
 15. Carrano, M. T., Benson, R. B. J., & Sampson, S. D. The phylogeny of Tetanurae (Dinosauria: Theropoda). *J. Syst. Palaeontol.* **10**, 211–300 (2012).
 16. Zanno, L. E., & Makovicky, P. J. Neovenatorid theropods are apex predators in the Late Cretaceous of North America. *Nat. Commun.* **4**(1), 1–9 (2013).
 17. Novas, F. E. *Megaraptor namunhuaiquii* gen. et. sp. nov., a large-clawed, Late Cretaceous Theropod from Argentina. *J. Vert. Pal.* **18**, 4–9 (1998).
 18. Apesteguía, S., Smith, N. D., Juárez Valieri, R., & Makovicky, P. J. An unusual new theropod with a didactyl manus from the Upper Cretaceous of Patagonia, Argentina. *PLoS One* **11** (7), e0157793 (2016).
 19. Porfiri, J. D., Juárez Valieri, R. D., Santos, D. D. D., & Lamanna, M. C. A new megaraptoran theropod dinosaur from the Upper Cretaceous Bajo de la Carpa Formation of northwestern Patagonia. *Cret. Res.* **89**, 302–319. <https://doi.org/10.1016/j.cretres.2018.03.014>. (2018)
 20. Lamanna, M. C., Casal, G.A., Martínez, R. D., & Ibiricu, L. M. Megaraptorid (Theropoda: Tetanurae) Partial Skeletons from the Upper Cretaceous Bajo Barreal Formation of Central Patagonia, Argentina: Implications for the Evolution of Large Body Size in Gondwanan Megaraptorans. *Ann Carnegie Mus.* **86**(3): 255–294 (2020)
 21. Azuma, Y., & Currie, P. J. A new carnosaur (Dinosauria: Theropoda) from the Lower Cretaceous of Japan. *Can. J. Earth Sci.* **37**(12):1735–1753. doi:10.1139/e00-064 (2000).
 22. Benson, R. B., Rich, T. H., Vickers-Rich, P., & Hall, M. Theropod fauna from southern Australia indicates high polar diversity and climate-driven dinosaur provinciality. *PLoS One* **7**(5), e37122 (2012).
 23. Poropat, S. F., White, M. A., Vickers-Rich, P., & Rich, T. H. New megaraptorid (Dinosauria: Theropoda) remains from the Lower Cretaceous Eumeralla Formation of Cape Otway, Victoria, Australia. *J. Vert. Pal.* **39**(4), e1666273 (2019).
 24. Bell, P. R., Cau, A., Fanti, F., & Smith, E. T. A large-clawed theropod (Dinosauria: Tetanurae) from the Lower Cretaceous of Australia and the Gondwanan origin of megaraptorid theropods. *Gond. Res.* **36**, 473–487 (2015).
 25. Brougham, T., Smith, E. T., & Bell, P. R. New theropod (Tetanurae: Avetheropoda) material from the 'mid'-Cretaceous Grimman Greek Formation at Lightning Ridge, New South Wales, Australia. *R. Soc. Open Sci.* **6**(1), 180826 (2019).
 26. Hocknull, S. A., White, M. A., Tischler, T. R., Cook, A. G., Calleja, N. D., Sloan, T., & Elliott, D. A. New Mid-Cretaceous (Latest Albian) Dinosaurs from Winton, Queensland, Australia. *PLoS One* **4**, e6190 (2009).
 27. Hocknull, S. A., Wilkinson, M., Lawrence, R. A., Konstantinov, V., Mackenzie, S., & Mackenzie, R. A new giant sauropod, *Australotitan cooperensis* gen. et sp. nov., from the mid-Cretaceous of Australia.

PeerJ **9**, e11317 (2021).

28. White, M. A., Bell, P. R., Poropat, S. F., Pentland, A. H., Rigby, S. L., Cook, A. G., Sloan, T., Elliott, D.A. New theropod remains and implications for megaraptorid diversity in the Winton Formation (lower Upper Cretaceous), Queensland, Australia. *R Soc Open Sci.* **7**(1):191462. doi:10.1098/rsos.191462 (2020).
29. Rolando, A. M. A., Egli, F. B., Sales, M. A., Martinelli, A. G., Canale, J. I., & Ezcurra, M. D. A supposed Gondwanan oviraptorosaur from the Albian of Brazil represents the oldest South American megaraptoran. *Cretac. Res.* **84**, 107–119 (2018).
30. Sales, M. A., Martinelli, A. G., Francischini, H., Rubert, R. R., Marconato, L. P., Soares, M. B., & Schultz, C. L. New dinosaur remains and the tetrapod fauna from the Upper Cretaceous of Mato Grosso State, central Brazil. *Hist. Biol.* **30**(5), 661–676 (2018).
31. Motta, M. J., Aranciaga Rolando, A.M., Rozadilla, S., Agnolín, F.E., Chimento, N.R., Brissón Egli, F., & Novas, F.E. New theropod fauna from the Upper Cretaceous (Huincul Formation) of northwestern Patagonia, Argentina. *Bull. N M. Mus. Nat. Hist. Sci.* **7**, 231e253 (2016).
32. Coria, R. A., & Currie, P.J. A New Megaraptoran Dinosaur (Dinosauria, Theropoda, Megaraptoridae) from the Late Cretaceous of Patagonia. *PLoS One* **11**(7), e0157973 (2016).
33. Sereno, P. C., Martínez, R. N., Wilson, J.A., Varricchio, D.J., & Alcober, O.A. Evidence for avian intrathoracic air sacs in a new predatory dinosaur from Argentina. *PLoS One* **3**, e3303 (2008).
34. Novas, F. E., Ezcurra, M. D., & Lecuona, A. *Orkoraptor burkei* nov.gen. et sp., a large theropod from the Maastrichtian Pari Aike Formation, Southern Patagonia, Argentina. *Cretac. Res.* **29**, 468e480 (2008).
35. Casal, G. A., Martínez, R. D., Luna, M. A. R. C. E. L. O., & Ibiricu, L. M. Ordenamiento y caracterización faunística del Cretácico Superior del Grupo Chubut, Cuenca del Golfo San Jorge, Argentina. *Rev. Bras. Paleontol.* **19**, 53–70 (2016).
36. Ibiricu, L. M., Casal, G. A., Martínez, R. D., Alvarez, B. N., & Poropat, S. F. New materials and an overview of Cretaceous vertebrates from the Chubut Group of the Golfo San Jorge Basin, central Patagonia, Argentina. *J. South Am. Earth Sci.* **98**, 102460 (2020).
37. Nullo, F. E., Blasco, G., Risso, C., Combina, A., & Otamendi, J. Hoja Geológica 5172-I y 5175-II El Calafate (2006).
38. Moyano-Paz, D., Rozadilla, S., Agnolín, F., Vera, E., Coronel, M. D., Varela, A. N.,... & Novas, F. E. The uppermost Cretaceous continental deposits at the southern end of Patagonia, the Chorrillo Formation case study (Austral-Magallanes Basin): Sedimentology, fossil content and regional implications. *Cret. Res.* **130**, 105059 (2022).
39. Hirasawa, T. The ligamental scar in the costovertebral articulation of the tyrannosaurid dinosaurs. *A. Palaeontol. Pol.*, **54**(1), 49–59 (2009).
40. Persons IV, W. S., & Currie, P. J. The tail of *Tyrannosaurus*: reassessing the size and locomotive importance of the *M. caudofemoralis* in non-avian theropods. *Anat. Rec.* **294**(1), 119–131 (2011).
41. Persons, W. S., Currie, P. J., & Norell, M. A. Oviraptorosaur tail forms and functions. *A. Palaeontol. Pol.* **59**(3), 553–567 (2013).

42. Madsen, J. H. *Allosaurus fragilis*: a revised osteology. Utah Geological and Mineral Survey, Utah Department of Natural Resources (1976).
43. Brochu, C. A. Osteology of *Tyrannosaurus rex*: insights from a nearly complete skeleton and high-resolution computed tomographic analysis of the skull. *J. Vert. Paleontol.* **22**(sup4), 1–138 (2003).
44. Currie, P. J., & Zhao, X. J. A new carnosaur (Dinosauria, Theropoda) from the Jurassic of Xinjiang, People's Republic of China. *Can. J. Earth Sci.* **30**(10), 2037–2081 (1993).
45. Lambe, L. M. The Cretaceous theropod dinosaur *Gorgosaurus* (No. **83**). Ottawa, Government printing bureau (1917).
46. Burch, S. H. Complete forelimb myology of the basal theropod dinosaur *Tawa hallae* based on a novel robust muscle reconstruction method. *J. Anat.* **225**(3), 271–297 (2014).
47. Schachner, E. R., Lyson, T. R., & Dodson, P. Evolution of the respiratory system in nonavian theropods: evidence from rib and vertebral morphology. *Anat. Rec.* **292**(9), 1501–1513 (2009).
48. Novas, F. E., Agnolín, F. L., Motta, M. J., & Brissón Egli, F. Osteology of *Unenlagia comahuensis* (Theropoda, Paraves, Unenlagiidae) from the Late Cretaceous of Patagonia. *Anat. Rec.* **304**:2741–2788 (2021).
49. Casal, G. A., Nillni, A. M., Valle, M. N., Svoboda, E. G., Tiedemann, C., Ciapparelli, H., ... & Luiz, M. M. Fossil-diagenesis in dinosaurs remains preserved in fluvial deposits of the Lago Colhué Huapi Formation (Upper Cretaceous), Golfo San Jorge Basin, Argentina. *Andean Geol.* **46**(3), 670-697 (2019).
50. Brusatte, S. L., & Benson, R. B. The systematics of Late Jurassic tyrannosauroid theropods from Europe and North America. *Act. Palaeontol. Pol.* **58**(1), 47–54 (2013).
51. Harris, J. D. *A Reanalysis of Acrocanthosaurus atokensis, its Phylogenetic Status, and Paleobiogeographic Implications, Based on a New Specimen from Texas: Bulletin 13 (Vol. 13)*. New Mexico Museum of Natural History and Science (1998).
52. Cuesta, E., Ortega, F., & Sanz, J. L. Axial osteology of *Concavenator corcovatus* (Theropoda; Carcharodontosauria) from the Lower Cretaceous of Spain. *Cret. Res.* **95**, 106–120 (2019).
53. Rauhut, O. W. A tyrannosauroid dinosaur from the Upper Jurassic of Portugal. *Palaeontol.* **46**(5), 903–910 (2003).
54. Wang, S., Stiegler, J., Amiot, R., Wang, X., Du, G. H., Clark, J. M., & Xu, X. Extreme ontogenetic changes in a ceratosaurian theropod. *Curr. Biol.* **27**(1), 144–148 (2017).
55. Martinelli, A. G., Borges Ribeiro, L. C., Méndez, A. H., Macedo Neto, F., Lourencini Cavellani, C., Felix, E., ... & de Paula Antunes Teixeira, V. Insight on the theropod fauna from the Uberaba Formation (Bauru Group), Minas Gerais State: new megaraptoran specimen from the Late Cretaceous of Brazil. *Riv. Ital. Paleontol. S.* **119** (2): 205-214 (2013).
56. Méndez, A. H., Novas, F. E., & Iori, F. V. First record of Megaraptora (Theropoda, Neovenatoridae) from Brazil. *C. R. - Palevol.* **11**(4), 251–256 (2012).

57. Lamanna, M. C., Casal, G. A., Martínez, R. D., & Ibiricu, L. M. Megaraptorid (Theropoda: Tetanurae) partial skeletons from the Upper Cretaceous Bajo Barreal Formation of central Patagonia, Argentina: implications for the evolution of large body size in Gondwanan megaraptorans. *Ann. Carnegie Mus.* **86**(3), 255–294 (2020).
58. White, M. A., Falkingham, P. L., Cook, A. G., Hocknull, S. A., & Elliott, D. A. Morphological comparisons of metacarpal I for *Australovenator wintonensis* and *Rapator ornitholestoides*: implications for their taxonomic relationships. *Alcheringa* **37**(4), 435–441 (2013).
59. O'Connor, P. M. Postcranial pneumaticity: an evaluation of soft-tissue influences on the postcranial skeleton and the reconstruction of pulmonary anatomy in archosaurs. *J. Morphol.* **267**(10), 1199–1226 (2006).
60. O'Connor, P. M., & Claessens, L. P. Basic avian pulmonary design and flow-through ventilation in non-avian theropod dinosaurs. *Nature* **436**(7048), 253–256 (2005).
61. Ezcurra, M.D., Novas, F.E. Theropod dinosaurs from Argentina. *Rev. Mus. Argentino Cienc. Nat., n.s.* **6**, 139–156 (2016).
62. Jacobs, L. L., & Winkler, D. A. Mammals, archosaurs, and the Early to Late Cretaceous transition in north-central Texas. *National Science Museum Monographs* **14**, 253–280 (1998).
63. Nesbitt, S. J., Denton, R. K., Loewen, M. A., Brusatte, S. L., Smith, N. D., Turner, A. H., ... Wolfe, D. G. A mid-Cretaceous tyrannosauroid and the origin of North American end-Cretaceous dinosaur assemblages. *Nat. Ecol. Evol.* **3**(6), 892–899 (2019).
64. Zanno, L. E., Tucker, R. T., Canoville, A., Avrahami, H. M., Gates, T. A., & Makovicky, P. J. Diminutive fleet-footed tyrannosauroid narrows the 70-million-year gap in the North American fossil record. *Commun. Biol.* **2**(1), 1–12 (2019).
65. Holtz Jr, T. R. Theropod guild structure and the tyrannosaurid niche assimilation hypothesis: implications for predatory dinosaur macroecology and ontogeny in later Late Cretaceous Asiamerica. *Can. J. Earth Sci.* **99**(999), 1–18 (2021).
66. Meso, J. G., Hendrickx, C., Baiano, M. A., Canale, J. I., Salgado, L., & Diaz-Martinez, I. Isolated theropod teeth associated with a sauropod skeleton from the Late Cretaceous Allen Formation of Río Negro, Patagonia, Argentina. *A. Palaeontol. Pol.* **66**(2), 409–423 (2021).
67. Cerroni, M. A., Motta, M. J., Agnolín, F. L., Rolando, A. A., Egli, F. B., & Novas, F. E. (2020). A new abelisaurid from the Huincul formation (Cenomanian-Turonian; upper Cretaceous) of Río Negro province, Argentina. *J. South Am. Earth Sci.* **98**, 102445 (2020).
68. Turner, A. H., Pol, D., Clarke, J. A., Erickson, G. M., & Norell, M. A. A basal dromaeosaurid and size evolution preceding avian flight. *Science* **317**(5843), 1378–1381 (2007).
69. Novas, F. E., Pol, D., Canale, J. I., Porfiri, J. D., & Calvo, J. O. A bizarre Cretaceous theropod dinosaur from Patagonia and the evolution of Gondwanan dromaeosaurids. *Proc. Royal Soc. B.* **276**(1659), 1101–1107 (2009).
70. DePalma, R. A., Burnham, D. A., Martin, L. D., Larson, P. L., & Bakker, R. T. The first giant raptor (Theropoda: Dromaeosauridae) from the hell creek formation. *Paleontological Contributions*

2015(14), 1–16 (2015).

71. Makovicky, P. J., Apesteguía, S., & Agnolín, F. L. The earliest dromaeosaurid theropod from South America. *Nature* **437**(7061), 1007–1011 (2005).
72. Motta, M. J., Agnolín, F. L., Egli, F. B., & Novas, F. E. New theropod dinosaur from the Upper Cretaceous of Patagonia sheds light on the paravian radiation in Gondwana. *Sci. Nat.* **107**(3), 1–8 (2020).
73. Gianechini, F. A., & Apesteguía, S. Unenlagiinae revisited: dromaeosaurid theropods from South America. *Anais Acad. Brasil. Ci.* **83**(1), 163–195 (2011).
74. Agnolín, F. L., Motta, M. J., Brissón Egli, F., Lo Coco, G., & Novas, F. E. Paravian phylogeny and the dinosaur-bird transition: an overview. *Front. Earth Sci.* **6**, 252 (2019).
75. Rauhut, O. W., & Werner, C. First record of the family Dromaeosauridae (Dinosauria: Theropoda) in the cretaceous of Gondwana (Wadi milk formation, northern Sudan). *Palaontol. Z.* **69**(3), 475–489 (1995).
76. Ely, R. C., & Case, J. A. Phylogeny of a new gigantic paravian (Theropoda; coelurosauria; maniraptora) from the upper cretaceous of James Ross Island, Antarctica. *Cret. Res.* **101**, 1–16 (2019).
77. Ibrahim, N., Maganuco, S., Dal Sasso, C., Fabbri, M., Auditore, M., Bindellini, G.,... Pierce, S. E. Tail-propelled aquatic locomotion in a theropod dinosaur. *Nature*, **581**(7806), 67-70 (2020).
78. Hone, D. W., & Holtz Jr, T. R. Evaluating the ecology of Spinosaurus: Shoreline generalist or aquatic pursuit specialist?. *Palaeontol Electron.* **24**(1), a03 (2021).
79. Novas, F., Dalla Vecchia, F., & Pais, D. Theropod pedal unguals from the Late Cretaceous (Cenomanian) of Morocco, Africa. *Rev. Mus. Argentino Cienc. Nat., n.s.* **7**(2), 167–175 (2005).
80. Novas, F. E. (2009). *The age of dinosaurs in South America*. Indiana University Press.
81. Bonaparte, J. F. The gondwanian theropod families Abelisauridae and Noasauridae. *Hist. Biol.* **5**(1), 1–25 (1991).
82. Novas, F. E. Alvarezsauridae, Cretaceous basal birds from Patagonia and Mongolia. *Mem. Queensl. Mus.* **39**, 675–702 (1996).
83. Novas, F. E. Anatomy of *Patagonykus puertai* (Theropoda, Avialae, Alvarezsauridae), from the late cretaceous of Patagonia. *J. Vert. Paleontol.* **17**(1), 137–166 (1997).
84. Agnolín, F. L., Powell, J. E., Novas, F. E., & Kundrát, M. New alvarezsaurid (Dinosauria, Theropoda) from uppermost Cretaceous of north-western Patagonia with associated eggs. *Cret. Res.* **35**, 33–56 (2012).
85. Delcourt, R., & Grillo, O. N. Tyrannosauroids from the Southern Hemisphere: Implications for biogeography, evolution, and taxonomy. *Palaeogeogr. Palaeoclimatol. Palaeoecol.* **511**, 379–387 (2018).
86. Qin, Z., Zhao, Q., Choiniere, J. N., Clark, J. M., Benton, M. J., & Xu, X. Miniaturization and Phylogenetic Radiation in Alvarezsauroids: Insights From Histological Analysis. *Available at SSRN 3765619*. (2021).

87. Novas, F. E., Ezcurra, M. D., Agnolin, F. L., Pol, D., & Ortíz, R. New Patagonian Cretaceous theropod sheds light about the early radiation of Coelurosauria. *Rev. Mus. Argentino Cienc. Nat.* **14**(1), 57–81 (2012).
88. Martínez, R., & Novas, F. *Aniksosaurus darwini* gen. et sp. nov., a new coelurosaurian theropod from the early Late Cretaceous of central Patagonia, Argentina. *Rev. Mus. Argentino Cienc. Nat., n.s.* **8**(2), 243–259 (2006).
89. Ibiricu, L. M., Martínez, R. D., Casal, G. A., & Cerda, I. A. The behavioral implications of a multi-individual bonebed of a small theropod dinosaur. *PLoS One* **8**(5), e64253 (2013).

Figures

A

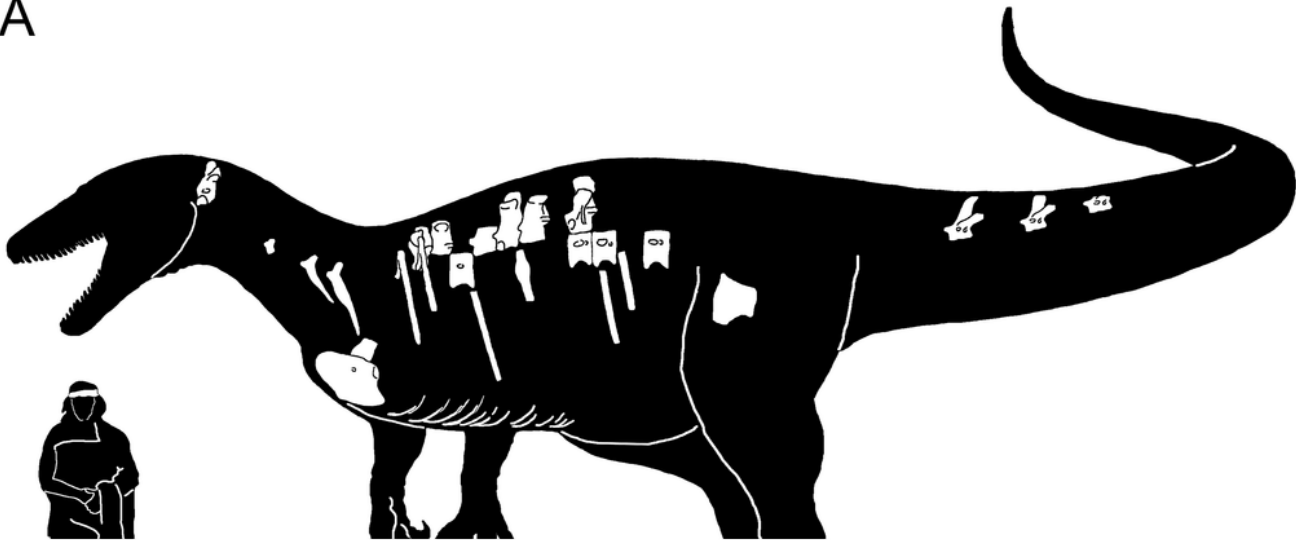


Figure 1

A, silhouette of *Maip macrothorax* showing the preserved bones in white. B, reconstruction of the thoracic cavity of *Maip*. C, interpretative drawing of the excavation of *Maip* showing the original disposition of the bones. Abbreviations: a, axis; c, coracoid; ind, indetermined bone; g, gastralia; r, rib; v, vertebrae.

Figure 2

Axis of *Maip* in lateral (A, A'), anterior (B, B'), posterior (C, C'), dorsal (D, D') and ventral (E, E'). Scale bar: 5 cms. Abbreviations: epi, epiphyses; ic, intercentrum; nc, neural canal; ns, neural spine; pl, pleurocoel; poz, postzygapophyses; pp, parapophyses; prz, prezygapophyses; tp, transverse process.

Figure 3

Second dorsal of *Maip*. Interpretative drawing showing the preserved parts of the bone (A, A') and lateral (B, B'), anterior (C, C'), posterior (D, D') and dorsal (E, E') views. Scale bar: 5 cms. Abbreviations: poz, postzygapophyses; pp, parapophyses; prz, prezygapophyses; tp, transverse process.

Figure 4

Third and fourth dorsals of *Maip*. Third dorsal, interpretative drawing showing the preserved parts (A, A'), lateral (B, B'), dorsal (C, C'), posterior (D, D') and ventral (E, E') views. Fourth dorsal in lateral (B, B'), anterior (C, C'), posterior (D, D') and dorsal (E, E') views. Scale bar: 5 cms. Abbreviations: pl, pleurocoel; poz, postzygapophyses; pp, parapophyses; tp, transverse process.

Figure 5

Fifth and sixth dorsals of *Maip*. Fifth dorsal, interpretative drawing showing the preserved parts (A, A'), lateral (C, C'), anterior (D, D') and dorsal (E, E') views. Sixth dorsal, interpretative drawing showing the preserved parts (B), lateral (F, F'), anterior (G, G'), posterior (H, H') and dorsal (I, I') views. Scale bar: 5 cms. Abbreviations: hys, hyosphene; hym, hypantrum; nc, neural canal; pn, pneumatophore; poz, postzygapophyses; pp, parapophyses; prz, prezygapophyses; tp, transverse process.

Figure 6

Seventh dorsal of *Maip*. Interpretative drawing showing the preserved parts (A, A'), lateral (B, B'), posterior (C, C'), dorsal (D, D') and ventral (E, E') views. Scale bar: 5 cms. Abbreviations: hym, hypantrum; pn, pneumatophore; poz, postzygapophyses; tp, transverse process.

Figure 7

Ninth dorsal of *Maip*. Left lateral (A, A'), anterior (B, B'), posterior (C, C'), right lateral (D, D') and dorsal (E, E') views. Scale bar: 5 cms. Abbreviations: hye, hyosphene; hym, hypantrum; nc, neural canal; ns, neural spine; pl, pleurocoel; pn, pneumatophore; poz, postzygapophyses; pp, parapophyses; prz, prezygapophyses; tp, transverse process.

Figure 8

Tenth or eleventh dorsal of *Maip*. Lateral (A, A'), anterior (B, B') and ventral (C, C') views. Scale bar: 5 cms. Abbreviations: pl, pleurocoel.

Figure 9

Caudal "A" (A-D) and caudal "B" (E-H) of *Maip*. Lateral (A, A', E, E'), anterior (B, B', F, F'), posterior (C, C', G, G') and dorsal (D, D', H, H') views. Scale bar: 5 cms. Abbreviations: af, accessory fossa; nc, neural canal; ns, neural spine; poz, postzygapophyses; prz, prezygapophyses; tp, transverse process.

Figure 10

Seventh (A-E) and eighth (F-H) cervical ribs of *Maip*. Seventh cervical rib in lateral (A, A'), medial (B, B'), ventral (C, C'), anterior (D, D') and posteromedial (E, E') views. Eighth cervical rib in lateral (F, F'), medial (G, G') and dorsal (H, H') views. Scale bars: 5 cms. Abbreviations: ap, anterior process; cap, capitulum; tub, tuberculum.

Figure 11

First (A-D), second (E-G) and sixth (H-J) dorsal ribs of *Maip*. First dorsal rib in anterior (A, A'), posterior (B, B') and proximal (C, C') views and close-up of the proximal end (D). Second dorsal rib in anterior (E, E'), posterior (F, F') and proximal (G, G') views. Sixth dorsal rib in anterior (H, H'), posterior (I, I') and medial (J, J') views. Scale bars: 5 cms. Abbreviations: ap, anterior process; cap, capitulum; pn, pneumatophore; tub, tuberculum.

Figure 12

Medial (A-D) and lateral (E-F) gastral elements of *Maip* in anterior (A, C, E) and dorsal (B, D, F) views. Scale bar: 5 cms. Abbreviations: alg, articulation surface for lateral gastral; amg, articulation surface for medial gastral.

Figure 13

Coracoid of *Maip* in lateral (A, A') and medial (B, B') views. Scale bar: 5 cms. Abbreviations: bt, biceps tubercle; cf, coracoid foramen; gl, glenoid; pvp, posteroventral process.

Figure 14

Reconstruction of costovertebral ligaments in dorsal vertebrae and rib of *Maip*. A, mid-dorsal vertebra showing the scars for costovertebral ligaments. Transverse process in dorsal (1) and ventral (2) views. Dorsal rib (3) in anterior view. Dorsal vertebra in lateral view (4-5). B, reconstruction of costovertebral ligaments (including the fibrous membrane) of a mid-dorsal segment. C, reconstruction of costovertebral ligaments (excluding the fibrous membrane) of the same segment. Figure not to scale. Abbreviations: dp, diapophysis; pp, parapophysis.

Figure 15

Phylogenetic relationships of *Maip* of the analysis with (A) and without (B) fragmentary taxa. Numbers represents Bremer values for each node.

Figure 16

Comparative drawings showing the features that supports Clade "A" (A-C) and Clade "B" (D-E). A, maxilar tooth of *Fukuiraptor* (A), *Australovenator* (A') and *Murusraptor* (A''). B, proximal end of tibia of *Australovenator* (B) and *Aerosteon* (B'). C, manual phalanx and close-ups of its flexor tubercles of *Fukuiraptor* (C), *Australovenator* (C') and *Megaraptor* (C''). D, dorsal vertebrae of *Murusraptor* (D) and *Tratayenia* (D'). E, dorsal view of a mid-caudal of *Megaraptor* (E) and *Maip* (E'). Abbreviations: af, accessory fossa; bl, bifurcated lamina; Imp, lateromedial platform; lms, lateromedial sulcus; md, mesial denticles; prz, prezygapophyses.

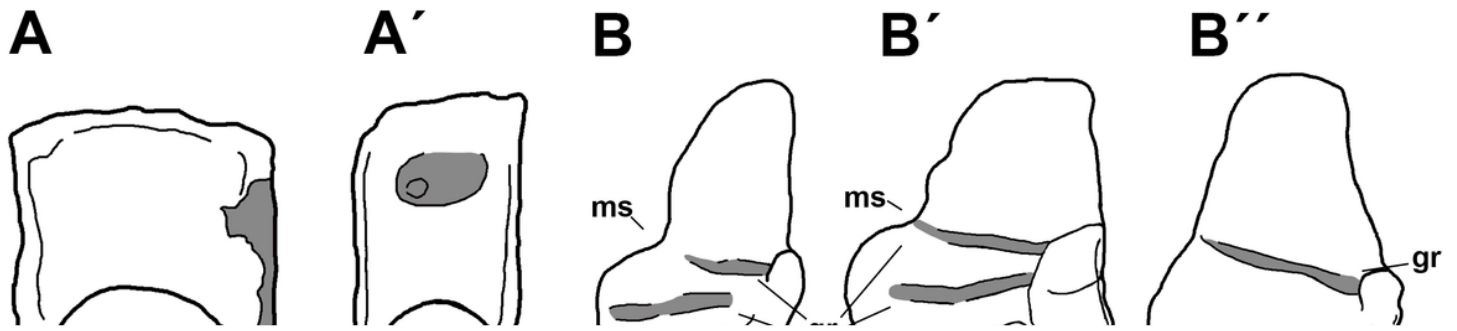


Figure 17

Comparative drawings of potential features supporting a natural clade of South American megaraptorids. A, dorsal vertebra of *Fukuiraptor* (A) and *Aerosteon* (A'). B, anterior view of astragalus of *Vayuraptor* (B), *Australovenator* (B') and *Aerosteon* (B''). C, dorsal (up) and distal (down) views of first of *Australovenator* (C), '*Rapator*' (C') and *Megaraptor* (C''). D, proximal view of ulna of *Australovenator* (D), a Megaraptoridae indet from Australia [NMV P186076] (D') and *Megaraptor* (D''). Abbreviations: gr, groove; lc, lateral condyle; lt, lateral tuberosity; lvp, lateroventral process; mc, medial condyle; ms, medial shelf; op, olecranon process; pvp, posteroventral process.

Figure 18

Phylogenetic relationships, chronostratigraphic implications, and body length of Megaraptora. A, Graphic illustrating temporal range of all known megaraptoran records and its importance in the fossils record compared with those of carcharodontosaurids. B, generalized phylogenetic relationships of Megaraptora, showing the Asian (black bars), Australian (red bars) and South American (blue bars) records, the main

synapomorphies supporting clades, the evolutionary trends and the presence of two different faunas within Australia (pink and purple areas). Tree topology follows the results of the present work. C, line showing the average size of megaraptorans within a certain time. D, graph showing the specific (dots) and average (lines) sizes of abelisaurids, megaraptorids and unenlagiids previous (continuous lines) and posterior (discontinuous lines) the Cenomanian-Turonian extinction event.

Supplementary Files

This is a list of supplementary files associated with this preprint. Click to download.

- [SupplementaryinformationI.docx](#)
- [SupplementaryinformationII.xlsx](#)
- [SupplementaryinformationIII.xlsx](#)